


RESEARCH ARTICLE

Open Access



Multi-analyte proteomic analysis identifies blood-based neuroinflammation, cerebrovascular and synaptic biomarkers in preclinical Alzheimer's disease

Xuemei Zeng¹, Tara K. Lafferty¹, Anuradha Sehrawat¹, Yijun Chen², Pamela C. L. Ferreira¹, Bruna Bellaver¹, Guilherme Povala¹, M. Ilyas Kamboh³, William E. Klunk¹, Ann D. Cohen¹, Oscar L. Lopez⁴, Milos D. Ikonovic^{1,4,5}, Tharick A. Pascoal¹, Mary Ganguli^{1,4,6}, Victor L. Villemagne¹, Beth E. Snitz⁴ and Thomas K. Karikari^{1*} 

Abstract

Background Blood-based biomarkers are gaining grounds for the detection of Alzheimer's disease (AD) and related disorders (ADRDs). However, two key obstacles remain: the lack of methods for multi-analyte assessments and the need for biomarkers for related pathophysiological processes like neuroinflammation, vascular, and synaptic dysfunction. A novel proteomic method for pre-selected analytes, based on proximity extension technology, was recently introduced. Referred to as the NULISAseq CNS disease panel, the assay simultaneously measures ~ 120 analytes related to neurodegenerative diseases, including those linked to both core (i.e., tau and amyloid-beta (A β)) and non-core AD processes. This study aimed to evaluate the technical and clinical performance of this novel targeted proteomic panel.

Methods The NULISAseq CNS disease panel was applied to 176 plasma samples from 113 individuals in the MYHAT-NI cohort of predominantly cognitively normal participants from an economically underserved region in southwestern Pennsylvania, USA. Classical AD biomarkers, including p-tau181, p-tau217, p-tau231, GFAP, NEFL, A β 40, and A β 42, were independently measured using Single Molecule Array (Simoa) and correlations and diagnostic performances compared. A β pathology, tau pathology, and neurodegeneration (AT(N) statuses) were evaluated with [¹¹C] PiB PET, [¹⁸F]AV-1451 PET, and an MRI-based AD-signature composite cortical thickness index, respectively. Linear mixed models were used to examine cross-sectional and Wilcoxon rank sum tests for longitudinal associations between NULISA and neuroimaging-determined AT(N) biomarkers.

Results NULISA concurrently measured 116 plasma biomarkers with good technical performance (97.2 \pm 13.9% targets gave signals above assay limits of detection), and significant correlation with Simoa assays for the classical biomarkers. Cross-sectionally, p-tau217 was the top hit to identify A β pathology, with age, sex, and APOE genotype-adjusted AUC of 0.930 (95%CI: 0.878–0.983). Fourteen markers were significantly decreased in A β -PET + participants, including TIMP3, BDNF, MDH1, and several cytokines. Longitudinally, FGF2, IL4, and IL9 exhibited A β PET-dependent yearly increases in A β -PET + participants. Novel plasma biomarkers with tau PET-dependent longitudinal changes

*Correspondence:

Thomas K. Karikari

Karikaritk@upmc.edu; karikari@pitt.edu

Full list of author information is available at the end of the article



© The Author(s) 2024. **Open Access** This article is licensed under a Creative Commons Attribution 4.0 International License, which permits use, sharing, adaptation, distribution and reproduction in any medium or format, as long as you give appropriate credit to the original author(s) and the source, provide a link to the Creative Commons licence, and indicate if changes were made. The images or other third party material in this article are included in the article's Creative Commons licence, unless indicated otherwise in a credit line to the material. If material is not included in the article's Creative Commons licence and your intended use is not permitted by statutory regulation or exceeds the permitted use, you will need to obtain permission directly from the copyright holder. To view a copy of this licence, visit <http://creativecommons.org/licenses/by/4.0/>. The Creative Commons Public Domain Dedication waiver (<http://creativecommons.org/publicdomain/zero/1.0/>) applies to the data made available in this article, unless otherwise stated in a credit line to the data.

included proteins associated with neuroinflammation, synaptic function, and cerebrovascular integrity, such as CHIT1, CHI3L1, NPTX1, PGF, PDGFRB, and VEGFA; all previously linked to AD but only reliable when measured in cerebrospinal fluid. The autophagosome cargo protein SQSTM1 exhibited significant association with neurodegeneration after adjusting age, sex, and APOE ϵ 4 genotype.

Conclusions Together, our results demonstrate the feasibility and potential of immunoassay-based multiplexing to provide a comprehensive view of AD-associated proteomic changes, consistent with the recently revised biological and diagnostic framework. Further validation of the identified inflammation, synaptic, and vascular markers will be important for establishing disease state markers in asymptomatic AD.

Keywords Preclinical Alzheimer's disease, Plasma biomarkers, Proteomics, Amyloid pathology, Tau pathology, Neurodegeneration, Nucleic acid-Linked Immuno-Sandwich Assay (NULISA), NULISA with next-generation sequencing readout (NULISAseq)

Background

The recent revision of the amyloid/tau/neurodegeneration (AT(N)) research framework emphasizes that Alzheimer's disease (AD) is a multifaceted disorder involving diverse brain pathologies and physiological processes [1]. In addition to A (β amyloid deposition), T (pathologic tau), and N (neurodegeneration) categories, which were included in the 2018 update [2], the recent update recommends biomarker assessments for inflammation (I) as well as mixed pathologies such as vascular (V) pathology and synucleinopathy (S). Furthermore, alteration of synapses can occur early in the AD continuum, even before overt neurodegeneration, making the examination of synaptic markers important in preclinical AD [3–5]. This new framework necessitates a diverse set of biomarkers for more accurate diagnosis, prognosis, clinical management, and development/evaluation of therapies. Analyses of multiple biomarkers integrated into a single test can enhance efficiency, reduce analytical errors, and save on specimen volume. However, multi-analyte assays that provide concurrent information on A, T, and N processes are lacking, let alone those that concomitantly include I, V, and S biomarkers. In fact, glial fibrillary acidic protein (GFAP) is the only marker listed under I, while V has no entry in terms of biofluid biomarkers recommended in the revision of the research and diagnostic framework [1].

Previous analyses of cerebrospinal fluid (CSF) implicated associations of several inflammatory, vascular, and synaptic function proteins with amyloid-beta ($A\beta$) and tau pathologies in AD. Regarding neuroinflammation, the astrocytic protein chitinase-3 like-protein-1 (CHI3L1), also known as YKL-40, has been shown to associate preferentially with tau pathology, while GFAP, a different astrocytic protein, was more strongly linked with $A\beta$ plaque pathology [6–9]. CSF levels of soluble TREM2, a transmembrane receptor protein predominantly expressed by microglia cells, were increased in AD and associated with tau-dependent neurodegeneration

and cognitive decline [10–13]. Levels of TREM1, another microglial transmembrane protein, were also shown to increase in AD dementia compared with cognitively unimpaired controls and those with mild cognitive impairment (MCI) [14]. In addition, multiple interleukins (ILs) in CSF were associated with $A\beta$ and tau abnormalities, as well as cognitive decline [15–20]. Similarly, several CSF markers of cerebrovascular integrity, such as soluble platelet-derived growth factor receptor β (PDGFRB), intercellular adhesion molecule 1 (ICAM1), vascular cell adhesion molecule 1 (VCAM1), and vascular endothelial growth factor (VEGFs), synaptic markers including neuronal pentraxin-1 (NPTX1) and neurogranin (NRGN), have been associated with AD and cognitive decline [18, 21–28]. High α -synuclein seed amplification assay positivity has been found in AD and is associated with atypical clinical manifestation [29].

A major challenge in the AD biomarker field is the difficulty in accurately measuring the aforementioned neuroinflammation, cerebrovascular, and synaptic protein markers in blood samples to give reliable performances as shown for their CSF counterparts. The development of blood-based assays for these biomarkers has been greatly impeded by several factors, including interference from the extremely complex blood proteome, low abundance of the target analytes, and signal attenuation by unwanted signal from peripheral sources [30, 31]. For example, assays for synaptic markers including NRGN give good analytical signals in plasma but without the corresponding good biomarker performance as shown in CSF [32, 33].

Recently, a highly multiplexed immunoassay capable of measuring classical AT(N) biomarkers alongside multiple I, V, and S biomarkers in plasma was described [34]. Known as the NULISAseq CNS disease panel, this assay employs an innovative automated technology called Nucleic acid-Linked Immuno-Sandwich Assay (NULISA). Coupling NULISA with next-generation sequencing readout (NULISAseq) allows detection of

hundreds of proteins with attomolar sensitivity and an ultra-broad dynamic range [34]. The NULISAseq CNS panel currently consists of ~120 protein targets covering the eight pathological hallmarks that define neurodegenerative diseases: namely, pathological protein aggregation, synaptic and neuronal network dysfunction, aberrant proteostasis, cytoskeletal abnormalities, altered energy homeostasis, DNA and RNA defects, inflammation, and neuronal cell death [35].

This study had a three-fold aim. Our first aim was to evaluate the technical performance of the NULISAseq CNS disease panel. For classical AT(N) biomarkers (e.g., p-tau181, p-tau217, p-tau231, A β 40, A β 42, GFAP, and neurofilament light chain [NEFL]), we compared the NULISA results with those obtained on the widely used Quanterix Single molecule array (Simoa). The second aim was to examine the diagnostic accuracies and longitudinal profiles of blood-based NULISAseq targets against neuroimaging measures of A, T and N in a population-based cohort of mostly cognitively normal older adults. Thirdly, we aimed to identify novel plasma I, V, and synaptic markers associated with A β positron emission tomography (PET), tau PET and magnetic resonance imaging (MRI)-based neurodegeneration measures in the same cohort.

Methods

Participants

The Monongahela Youghiogheny Healthy Aging Team-Neuroimaging (MYHAT-NI) is a sub-cohort of the parent MYHAT study, a population-based prospective study of cognitively normal older adults designed to characterize the prevalence of MCI in older adults with a low socioeconomic status in selected Rust Belt regions in southwestern Pennsylvania, USA [36–38]. The MYHAT study recruited participants aged 65 and older via age-stratified random sampling from publicly available voter registration lists. The MYHAT-NI study included a subset of MYHAT participants with a Clinical Dementia Rating (CDR) sum-of-box score [39] of <1.0 for neuroimaging assessments to investigate the distribution and functional correlates of AD. For this reason, all MYHAT-NI participants had normal (CDR=0) or only very mildly impaired cognition (CDR=0.5) at the time of enrollment which started in 2017. The only exclusion criterion was contraindication to neuroimaging. The study had two visits: baseline and approximately two-year follow-up. Sociodemographic information was collected at the baseline visit. Both racial identity and years of education were self-reported. Blood collection, neurophysiological assessment, and neuroimaging, including [^{11}C] Pittsburgh Compound B (PiB) PET imaging of A β plaques, [^{18}F] AV-1451 PET imaging of tau pathology, and structural

MRI for neurodegeneration, were performed at both baseline and the follow-up visits following standard protocols [40–42]. Detailed study designs for MYHAT and MYHAT-NI, including participant recruitment strategies, multi-domain cognitive assessments, neuroimaging, and data processing, can be found in previous publications [36, 38]. *APOE* genotyping was determined as previously described [43].

We classified A, T, and N status according to [^{11}C] PiB PET, [^{18}F] AV-1451 PET, and MRI scans for cortical thickness, respectively. The A status was based on a global [^{11}C] PiB standardized uptake value ratio (SUVR) computed by volume-weighted averaging of nine composite regional outcomes (anterior cingulate, posterior cingulate, insula, superior frontal cortex, orbitofrontal cortex, lateral temporal cortex, parietal, precuneus, and ventral striatum) [41]. Participants were classified as A+ or A- based on a pre-defined cutoff, with >1.346 as A+ [44, 45]. For T status, a composite SUVR was computed for each [^{18}F] AV-1451 PET by normalizing composite Braak regional values ((Braak I–VI) to FreeSurfer cerebellar gray matter activity [46, 47]. Participants with SUVR >1.18 were considered T+, <=1.18 as T- [48]. N status was based on an AD-signature composite cortical thickness index derived from a surface-area weighted average of the mean cortical thickness of four FreeSurfer regions of interest (ROIs) – entorhinal, inferior temporal, middle temporal, and fusiform – that are most predictive of AD-specific diagnosis and pathology, with <2.7 as N+ [44, 49]. The MYHAT-NI study was approved by the University of Pittsburgh Institutional Review Board (STUDY19020264).

NULISAseq assay procedures and data processing

Plasma samples were sent to Alamar Biosciences, Inc. for NULISAseq measurements. Alamar Biosciences also provided all the reagents for the NULISAseq assay. The analysis was conducted blinded, with Alamar Biosciences, Inc. unaware of the sample grouping information until after the analysis had been completed. The content of the CNS panel was based on suggestions from multiple experts in CNS disease drug development and biomarker research. It includes both established and emerging biomarkers of neurodegenerative diseases that represent multiple hallmarks of neurodegenerative diseases. For ease of cross-reference, all NULISAseq biomarkers were represented using non-italicized upper-case gene symbols as used by the vendor. Italicized upper-case symbols were used when referring to genes. The complete list of biomarkers with their full protein names and gene symbols included in the NULISAseq panel is provided in Additional file 1.

Plasma samples were thawed and centrifuged at 10,000xg for 10 min to remove particulates. The supernatants were then analyzed using the NULISAseq CNS disease panel on an Alamar ARGO™ prototype system, as previously described [34]. In brief, samples were incubated with a cocktail of paired capture and detection antibodies for the included target protein biomarkers and the internal control (IC). The capture antibodies were conjugated with partially double-stranded DNA containing a poly-A tail and a target-specific barcode, while detection antibodies were conjugated with another partially double-stranded DNA containing a biotin group and a matching target-specific barcode. After incubation, the mixtures underwent magnetic bead-based capture, wash, release, recapture, and a second round of wash processes to purify the formed immunocomplexes. A ligation mix, including T4 DNA ligase and a specific DNA ligator sequence, was utilized to ligate the proximal ends of DNA attached to the paired antibodies, generating DNA reporter molecules containing unique target and sample-specific barcodes. The reporter DNA levels were then quantified by Next-Generation Sequencing (NGS). The plasma samples were randomized in two plates for the assay. Three assay controls were run side-by-side with samples for each plate, including the sample control (2 replicates/plate), the inter-plate control (IPC; 3 replicates/plate), and the negative control (2–3 replicates/plate).

Data normalization was performed to remove potential unwanted technical variation. First, IC-based normalization was done by dividing the target counts for each sample well by that well's IC counts. IPC normalization was achieved by dividing IC-normalized counts by target-specific medians of the IPC (pooled plasma) sample replicates on that plate. Finally, the data was rescaled and log₂-transformed to give a more normal distribution for subsequent statistical analyses. These values are hereafter referred to as NULISA Protein Quantification (NPQ) units. The fold change difference between two groups were calculated as $2^{(\text{difference in NPQ})}$. The plate-specific limit of detection (LOD) was calculated for each target assay by taking the mean plus three times the standard deviation (SD) of the unlogged normalized counts for the negative control samples on the plate. LODs were then rescaled and log₂-transformed as above. Measurements for sample controls were used to evaluate the reproducibility of the assays, including both the within-run and between-run coefficients of variation (CVs).

Procedures for Simoa assays

Simoa assays were performed on an HD-X instrument (Quanterix, Billerica, MA, USA). Prior to the measurements, plasma samples were thawed at room temperature

and centrifuged at 4000xg for 10 min to remove particulates. Plasma NEFL, GFAP, Aβ₄₂ and Aβ₄₀ were measured with the Neurology 4-Plex E (#103670), p-tau181 with the p-tau181 V2 Advantage kit (#103714), and p-tau217 with the ALZpath Simoa® p-Tau 217 V2 Assay Kit (#104371). Quality control (QC) samples of 2–3 different concentrations for each assay were analyzed at the start and the end of each run to assess the reproducibility of each assay. The average within-run CVs of the QC samples were 3.7% for p-tau217, 6.6% for p-tau181, 14.3 for NEFL, 9.9% for GFAP, 8.9% for Aβ₄₂, and 9.5% for Aβ₄₀. The average between-run CVs were 11.4% for p-tau217, 11.7% for p-tau181, 18.3% for NEFL, 17.8% for GFAP, 13.0% for Aβ₄₂, and 14.6% for Aβ₄₀.

Statistical analysis

All analyses were conducted using MATLAB (version R2021b) or R statistical software version 4.2.1 (R Foundation for Statistical Computing, Vienna, Austria; <http://www.r-project.org/>). We utilized the Wilcoxon rank-sum test for two-group comparisons and the Kruskal–Wallis test for comparisons involving more than two groups. Spearman's rank correlation was used to measure the strength and direction of association between two continuous variables. For demographic characteristics, continuous variables were presented as median and interquartile range (IQR), while categorical variables were reported as counts. Wilcoxon rank-sum tests and Fisher's exact tests were employed to assess the significance of differences between A+ and A- participants for continuous and categorical variables, respectively. Linear mixed models were used to assess the association of common AD risk factors, including age, sex, and *APOE* ε4 carrier status, with biomarkers.

The following statistical tests were applied to evaluate cross-sectional associations between plasma biomarkers and brain Aβ and tau pathologies: (1) Wilcoxon rank-sum tests for the univariate significance for the associations between NPQs and dichotomous pathology variables (e.g., A- vs. A+), without adjusting for risk factors; (2) Spearman's rank correlation to measure the strength and direction of the associations between NPQs and continuous variables (e.g., Aβ PET SUVR); (3) linear mixed models (random intercepts) with biomarker NPQs as the dependent variable, visit-specific Aβ PET status as the independent variables, as well as common risk factors (such as age, sex and *APOE* ε4 carrier status) to determine the overall risk factor-adjusted significance combining samples from both visits. False discovery rate corresponding to cutoff *p*-values were calculated according to the procedure described by Yoav Benjamini and Yosef Hochberg in 1995 [50]. An arbitrary *p*-value of 0.005 was used as the significance cutoff, which

corresponded to 3 to 10% FDR depending on the comparisons. Receiver operating characteristic (ROC) curves and the area under curve (AUC) were calculated using the MATLAB *perfcurve* function, based on scores predicted from generalized linear regression models fitted using the MATLAB *fitglm* function. Confidence intervals were computed using bootstrap with 1000 replicates. DeLong test implemented in the pROC package was used to compare ROC curves [51, 52]. Web app VolcanoR was used to draw the volcano plot [53].

Longitudinal analysis was limited to participants with plasma samples analyzed at both visits. We calculated the yearly percentage of change for biomarker NPQs and continuous AD pathology variables using this formula: $100 * ([\text{Follow up} - \text{Baseline}] / [\text{Baseline}]) / \Delta \text{Time}$ in years. Wilcoxon rank-sum tests were then used for two-group comparisons, and Spearman's rank correlation to assess the association between yearly plasma biomarker changes and the annual A or T pathology change. Due to the relatively short duration between the two visits, we did not expect drastic changes in both blood and neuroimaging biomarker levels. Therefore, we treated the longitudinal analysis as explorative, and the original rather than FDR-adjusted *p*-values were used to determine significance.

Results

Cohort characteristics

This study comprised 176 plasma samples from 113 participants (average age 76.7 years at baseline, 54.0% women, and 95.0% non-Hispanic White) from the MYHAT-NI cohort (see Table 1 for demographic characteristics). These participants were recruited from the parent MYHAT cohort, which includes areas with relatively low socioeconomic status. The median Area Deprivation Index (ADI) in the MYHAT study area is at the 85th percentile nationally, according to the Neighborhood Atlas [54]. Among them, 63 participants (55.8%) provided plasma samples at two visits (baseline and the 2-year visit). At baseline, 85 (75.2%) participants were classified as A β -negative (A-) and 28 (24.8%) as A β -positive (A+), while 42 (66.7%) and 21 (33.3%) were A- and A+, respectively at the 2-year visit. Regarding tau PET, 74 (65.4%) participants were tau-negative (T-) and 39 (34.5%) as tau-positive (T+) at baseline. At the 2-year visit, 42 (66.7%) participants were T-, and 21 (33.3%) were T+. In terms of neurodegeneration according to cortical thickness, 80 (70.8%) participants were considered N- and 33 (29.2%) N+ at baseline, while at the 2-year visit, there were 42 (66.7%) N- and 20 (31.7%) N+ participants. One participant had missing N status at the 2-year visit due to poor MRI quality.

Most participants were cognitively normal at both visits. CDR-based cognitive assessment rated 102 participants (90.2%) as cognitively normal (CDR=0) and 10 (8.9%) as mildly impaired (CDR=0.5) at baseline. At the 2-year visit, 54 participants (85.7%) were cognitively normal, and 5 (7.9%) were mildly impaired. One participant at baseline and four at the 2-year visit missed CDR assessments. Similar results were obtained based on Mini-Mental State Examination (MMSE) assessment. Out of 112 participants with MMSE assessment at baseline, 108 (96.4%) participants were cognitively normal (MMSE \geq 24), and 4 (3.6%) were mildly impaired (MMSE between 19 – 23). All participants with MMSE assessment at the 2-year visit (38 out of 63) were cognitively normal.

Technical performance and head-to-head comparison of the NULISaseq measurements with Simoa assays

A total of 116 target assays were incorporated in the NULISaseq CNS disease panel for this study. The plasma concentration range of these targets spanned a minimum of 6 orders of magnitude according to the concentration estimated by mass spectrometry-based proteomics in the Human Protein Atlas database [55, 56]. Despite the broad dynamic ranges of the protein targets, the vast majority exhibited very high detectability, defined as the percentage of samples above the LOD, with a mean \pm SD detectability of $97.2\% \pm 13.9\%$ (Fig. 1A). Only three targets – UCHL1 (ubiquitin C-terminal hydrolase L1), PTN (pleiotrophin), and pTDP43-409 (transactive response DNA binding protein of 43 kDa [TDP43] phosphorylated at Ser409) – had detectability below 70%. The median intra-plate and inter-plate CVs were 4.34% (IQR: 2.80%–6.04%) and 3.11% (IQR: 1.41%–5.45%), respectively, suggesting robust assay reproducibility (Fig. 1B and C). Only two targets – CNTN2 (contactin 2) and NEFH (neurofilament heavy chain) – had inter-plate CVs greater than 20%, a cutoff commonly used for in vitro diagnostic assays. To assess whether the variation depended on protein abundance, we evaluated the association between the intra- or inter-plate CVs and the abundance ranks for targets ($n=46$) with plasma concentration data available from the Human Protein Atlas database. As depicted in Fig. 1D and E, both intra- and inter-plate CVs were not influenced by protein abundance, with *p*-values for Spearman rank correlations being 0.173 and 0.919, respectively.

We next examined the correlation between NULISaseq measurements and Simoa measurements of selected biomarkers. These included p-tau217, p-tau231, p-tau181, GFAP, NEFL, A β 40, and A β 42. Notably, strong correlations were observed in all pairwise comparisons, with Spearman rank correlation coefficient (*r* ρ) values

Table 1 Participant characteristics in the MYHAT-NI cohort

	MYHAT-NI (Baseline)				MYHAT-NI (2-year visit)			
	Total	A β PET –	A β PET +	<i>p</i> -value ^a	Total	A β PET –	A β PET +	<i>p</i> -value ^a
N (%)	113	85 (75.2%)	28 (24.8%)		63	42 (66.7%)	21 (33.3%)	
Age (years)	76.0 (72.0 – 80.3)	75.0 (71.0 – 79.3)	79.0 (73.5 – 82.5)	0.055	77.0 (74.0 – 81.8)	76.0 (74.0 – 81.0)	78.0 (73.8 – 82.3)	0.884
Sex				0.275				0.109
Female (%)	61	43 (70.5%)	18 (29.5%)		32	18 (56.3%)	14 (43.7%)	
Male (%)	52	42 (80.8%)	10 (19.2%)		31	24 (77.4%)	7 (22.6%)	
Education (years)	12 (12 – 16)	12 (12 – 16)	13 (12 – 15)	0.583	13 (12 – 16)	14 (12 – 16)	12 (12 – 14)	0.050
Years between visits					2.4 (2.2 – 2.6)	2.4 (2.2 – 2.6)	2.4 (2.2 – 2.7)	0.358
Race				1.000				1.000
Non-Hispanic White	107	80 (74.8%)	27 (25.2%)		60	40 (66.7%)	20 (33.3%)	
Black/African American	6	5 (83.3%)	1 (16.7%)		3	2 (66.7%)	1 (33.3%)	
MMSE^b				0.430				1.000
> = 24	108	81 (75.0%)	27 (25.0%)		38	26 (68.4%)	12 (31.6%)	
19–23	4	3 (7.0)	1 (25.0%)		0	0	0	
CDR^c				0.015				0.033
CDR = 0	102	80 (78.2%)	22 (21.8%)		54	39 (72.7%)	15 (27.3%)	
CDR = 0.5	10	4 (40.0%)	6 (60.0%)		5	(20.0%)	4 (80.0%)	
APOE ϵ4 carrier				< 0.001				0.014
Yes	18	6 (33.3%)	12 (66.7%)		12	4 (33.3%)	8 (66.7%)	
No	95	79 (83.2%)	16 (16.8%)		51	38 (74.5%)	13 (25.5%)	
Tau PET^d				< 0.001				0.001
Negative	74	65 (87.8%)	9 (12.2%)		42	34 (81.0%)	8 (19.0%)	
Positive	39	20 (51.3%)	19 (48.7%)		21	8 (38.1%)	13 (61.9%)	
N Status^e				0.639				0.395
Negative	80	59 (73.8%)	21 (26.3%)		42	26 (61.9%)	16 (38.1%)	
Positive	33	26 (78.8%)	7 (21.2%)		20	15 (75.0%)	5 (25.0%)	

The median and interquartile range (IQR) are reported for continuous variables. Frequencies and percentages are shown for categorical variables. ^a*P*-values were calculated using the Wilcoxon rank-sum test for a continuous variable and Fisher's exact test for a categorical variable, respectively. ^bOne participant at baseline and 25 at the 2-year visit had missing MMSE assessment. ^cOne participants at baseline and 4 at the 2-year visit missed CDR assessment. ^d[¹⁸F]AV-1451 PET, Mean SUVR > 1.18 as positive. ^eN status is based on cortical thickness, with < 2.7 being positive. One A β PET- participant missed MRI for 2-year visit. Both racial identity and education were self-reported

(See figure on next page.)

Fig. 1 Technical performance of the NULISAseq CNS disease panel. **A** Box plots illustrating the detectability of 116 targets in 176 plasma samples collected from 113 MYHAT-NI participants. The y-axis represents NPQ-LOD, where values > 0 indicate detectability. For each box plot, the central mark indicates the median, and the bottom and top edges of the box indicate the 25th and 75th percentiles, respectively. The whiskers extend to the most extreme data points not considered outliers, and the outliers are plotted individually using the '+' marker symbol. Data points were considered outliers if they were greater than $q_3 + 1.5 \times (q_3 - q_1)$ or less than $q_1 - 1.5 \times (q_3 - q_1)$, where q_1 and q_3 are the 25th and 75th percentiles of the sample data. **B-C** Histogram distributions of intra-plate (**B**) and inter-plate (**C**) coefficient of variations (CVs). **D-E** Scatterplot distributions between abundance rank and intra-plate (**D**) or inter-plate (**E**) CVs. Intra- and inter-plate CVs were calculated based on results of a pooled plasma sample (SC), measured in duplicates separately in two different plates. Abundance rank was based on the mass spectrometry-estimated protein abundance in the Human Protein Atlas (downloaded on 12/24/2023). **F** Scatterplot distributions illustrating the correlation of protein levels measured using NULISAseq and Simoa method. *Rho* and *p* values were determined using Spearman rank-based correlation. Purple lines indicated the least square regression lines. Abbreviations: NPQ, NULISA Protein Quantification, represents the log₂-transformation of normalized target counts; LOD, limit of detection. Simoa measured concentration (fg/ml) was also log₂-transformed for this analysis

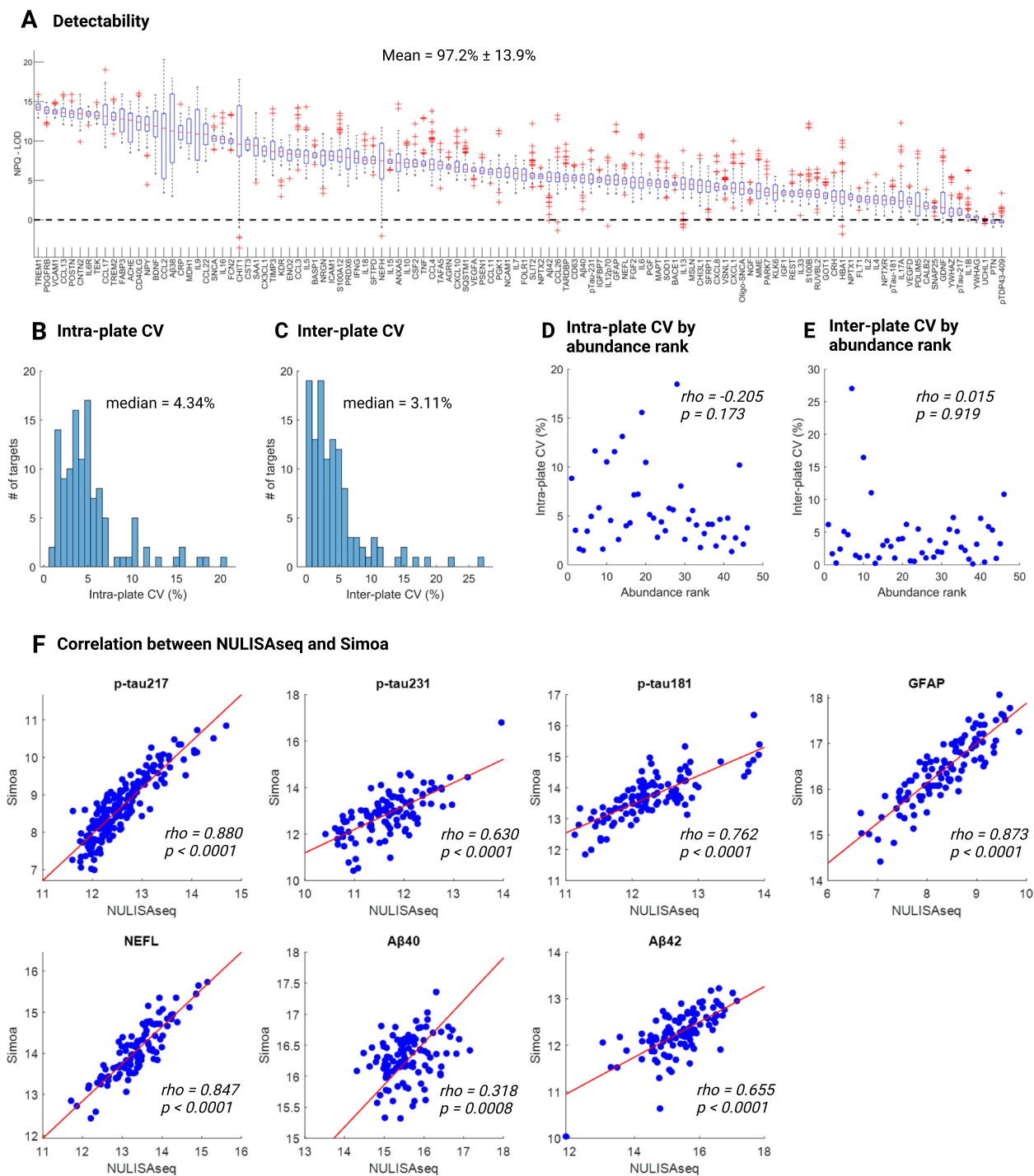


Fig. 1 (See legend on previous page.)

spanning from 0.318 to 0.880 (Fig. 1F). P-tau217, GFAP, and NEFL demonstrated the strongest between-platform correlation, with ρ of 0.880, 0.873, and 0.847, respectively.

To compare the diagnostic accuracies of the two measurements in detecting Aβ PET positivity, we calculated

the ROC AUCs using logistic regression models in the baseline samples (Table 2). NULISaseq demonstrated comparable performance to Simoa for all seven biomarkers, irrespective of whether common risk factors (age, APOE ε4 carrier status, and sex) were included in the models. For example, at baseline, plasma p-tau217 had

Table 2 Diagnostic accuracy (ROC analysis) of NULISAseq and Simoa biomarkers for A β PET positivity

AUC (95% CI)	ROC AUC with Biomarker only			ROC AUC with Biomarker + risk factors		
	NULISAseq	Simoa	<i>p</i> -value	NULISAseq	Simoa	<i>p</i> -value
p-tau217	0.905 (0.841–0.969)	0.880 (0.800–0.959)	0.625	0.930 (0.878–0.983)	0.925 (0.874–0.977)	0.891
p-tau231	0.718 (0.615–0.822)	0.632 (0.517–0.746)	0.274	0.806 (0.709–0.903)	0.790 (0.689–0.891)	0.822
p-tau181	0.576 (0.468–0.684)	0.669 (0.560–0.778)	0.237	0.780 (0.678–0.882)	0.793 (0.662–0.893)	0.867
GFAP	0.732 (0.640–0.825)	0.743 (0.653–0.834)	0.867	0.808 (0.717–0.899)	0.816 (0.725–0.908)	0.901
NEFL	0.565 (0.442–0.688)	0.599 (0.480–0.719)	0.695	0.766 (0.655–0.878)	0.791 (0.682–0.901)	0.755
A β 40	0.539 (0.409–0.669)	0.650 (0.530–0.771)	0.221	0.773 (0.670–0.875)	0.816 (0.719–0.913)	0.547
A β 42	0.531 (0.411–0.650)	0.550 (0.432–0.667)	0.826	0.779 (0.671–0.886)	0.789 (0.691–0.887)	0.884

Risk factors included age as a numeric variable, sex (male and female), and *APOE* status (*APOE* ϵ 4 carrier or non-carrier). The confidence interval of AUC was computed using the bootstrapping approach. *P*-value was determined using the DeLong test implemented in the pROC package in RStudio

AUCs of 0.905 (95% CI: 0.841–0.969) on NULISA and 0.880 (95% CI: 0.800–0.959) on Simoa. When accounting for risk factors, these AUCs increased to 0.930 (95% CI: 0.878–0.980) and 0.925 (95% CI: 0.874–0.977). The DeLong test showed no significant difference between the AUCs. These findings suggest that despite its highly multiplexed nature, the NULISAseq platform performs equivalently as Simoa for quantifying these biomarkers.

Association of NULISAseq targets with PET measure of amyloid pathology (A)

Cross-sectional association

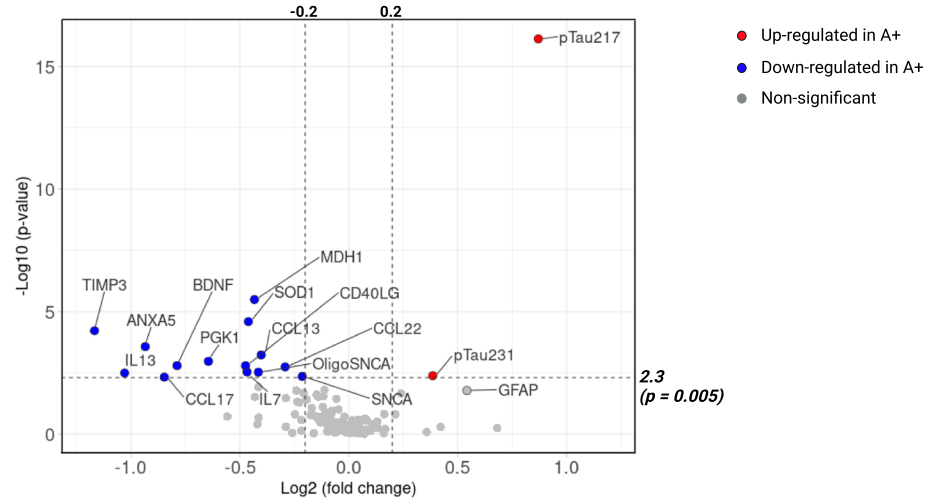
Several NULISAseq targets showed significant association with the common AD risk factors age, sex, and *APOE* ϵ 4 carrier status (Additional file 2: Figure S1). To account for the potential confounding effect of these risk factors, we utilized linear mixed models, to evaluate the adjusted significance for the cross-sectional association between NULISAseq targets and neuroimaging biomarkers.

A total of 16 targets showed significant association with A β pathology, as determined by A β PET, according to *p*-value < 0.005, corresponding to approximately 8% FDR (Fig. 2A). Figure 2B illustrates boxplot distributions of significant targets at baseline and the 2-year visit. As stated above, NULISAseq plasma p-tau217 demonstrated superior diagnostic accuracy in detecting A β PET positivity, achieving AUCs of 0.905 (95% CI: 0.841–0.969) and 0.922 (95% CI: 0.825–0.972) at the baseline and 2-year visits, respectively, when utilized as the sole predictor. Incorporating the risk factors age, sex, and *APOE* ϵ 4 carrier status raised the AUCs to 0.930 (95% CI: 0.878–0.983) and 0.938 (95% CI: 0.856–0.979), respectively. On average, A+ participants exhibited an 82.8% elevation in plasma p-tau217 levels compared with A- controls. NULISAseq p-tau231 also exhibited significant association. However, the AUCs and fold increases were inferior to plasma p-tau217. The AUCs were 0.718

(95% CI: 0.615–0.822) in the baseline and 0.698 (95% CI: 0.556–0.821) in the 2-year samples based on biomarker-only models, which increased to 0.808 (95% CI: 0.717–0.899) and 0.794 (95% CI: 0.652–0.888) respectively, with the inclusion of the risk factors. An overall 30.7% increase was observed comparing p-tau231 levels in A+ participants to those in A- controls. Moreover, GFAP showed high univariate association prior to adjusting for common risk factors, with Wilcoxon rank-sum *p*-values of 0.0002 for the baseline and 0.006 for the 2-year cohort. However, GFAP showed a strong association with age and *APOE* ϵ 4 carrier status (Additional file 2: Figure S1B and S1C), and its risk factor-adjusted significance weakened to a *p*-value of 0.016. The fold increase of GFAP in A+ vs. A- participants was 45.7%. It distinguished A+ from A- participants with AUCs of 0.732 (95% CI: 0.640–0.825) and 0.715 (95% CI: 0.569–0.830) in the baseline and 2-year cohorts based on biomarker-only models, and 0.808 (95% CI: 0.717–0.899) and 0.815 (95% CI: 0.668–0.926), respectively, after adjusting for common risk factors.

Contrarily, the other targets that showed significant associations with A β pathology demonstrated decreased protein levels in the A+ versus A- participants (Fig. 2A and B). Metalloproteinase inhibitor 3 (TIMP3), a metalloprotease inhibitor involved in regulating proteostasis [57, 58], exhibited the most substantial decrease in protein levels, with a 60%-fold decrease in A+ vs. A- individuals. TIMP3 distinguished A+ and A- participants with AUCs of 0.711 (95% CI: 0.596–0.814) and 0.739 (95% CI: 0.574–0.859) for the baseline and 2-year visit cohorts when used as the sole predictor. The inclusion of common risk factors improved the AUCs to 0.850 (95% CI: 0.718–0.923) and 0.882 (95% CI: 0.757–0.946). Malate dehydrogenase subunit 1, MDH1, also emerged as one of the top significant proteins, with the risk factor-adjusted *p*-value < 0.0001, and decreased at an average of 26% in A+ participants. BDNF, a neurotrophic factor

A Association between NULISaseq targets and Aβ PET



B Significant NULISaseq targets

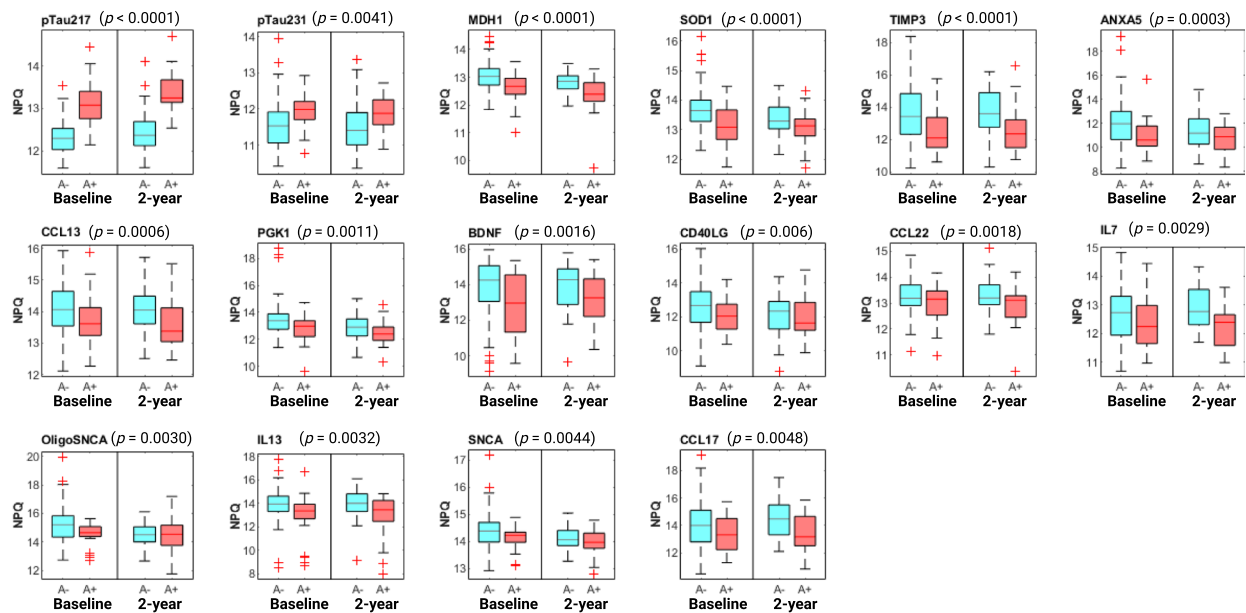


Fig. 2 Cross-sectional association of NULISaseq targets with amyloid pathology (A). **A** Volcano plot of $-\log_{10}(p\text{-value})$ versus $\log_2(\text{fold change})$ comparing biomarker abundances (NPQ) in samples from A+ participants ($n = 49$) vs. A- controls ($n = 127$). Significant targets are shown in red (higher in A+) or blue (lower in A+) circles. Grey circles represent non-significant targets. NPQ (NULISA Protein Quantification) represents the \log_2 -transformation of normalized target counts. **B** Boxplot distributions of significant NULISaseq targets, separated by A status and visit. P-values on top of the boxplots were for the whole data combining both visits and were determined using linear mixed models (random intercepts) with NPQs as the dependent variable, visit-specific A status as the independent variables, adjusting for covariates age, sex, and APOE $\epsilon 4$ carrier status. Significance determination was based on $p\text{-value} < 0.005$, corresponding to $\sim 8\%$ FDR

with pivotal roles in regulating synaptic plasticity and neuronal survival, showed an overall 42% reduction in A+ participants.

Six cytokines—IL7, IL13, CD40LG, CCL13, CCL17, and CCL22—were significantly associated with Aβ pathology, supporting the involvement of immune

response and inflammation in AD. Additional significant targets included superoxide dismutase 1 (SOD1), phosphoglycerate kinase 1 (PGK1), annexin A5 (ANXA5), and NULISaseq targets for soluble α -synuclein (SNCA) and oligomeric α -synuclein (OligoSNCA).

Longitudinal association

We then investigated the longitudinal relationship between NULISaseq targets and A β pathology. Three cytokines – FGF2, IL4, and IL9 – exhibited A β PET-dependent yearly percentage changes, with Wilcoxon rank-sum test *p*-values of 0.02, 0.04, and 0.04, respectively (Fig. 3A). The median yearly percentage changes were 9.1%, 1.5%, and 15.4% in A+ individuals, compared to -12.8%, -9.5%, and 0.4% in A- participants, respectively, for FGF2, IL4, and IL9. This means that while the cytokine levels increased over time in A+ individuals, large decreases were recorded for A- participants.

Next, we explored the influence of baseline biomarker levels on the progression of A β pathology, defined as the yearly percentage change in A β PET SUVR. Apart from p-tau217, five chemokines – CCL26, CCL17, CCL13, CXCL1, and CXCL8 – demonstrated significant associations (Fig. 3B). Higher baseline levels of p-tau217 were associated with more robust increases in A β PET

SUVR, with Spearman *rho* of 0.367 (*p*=0.003). On the contrary, elevated baseline levels of all five chemokines were linked with a smaller A β PET SUVR increase, with *rho* of -0.363 (*p*=0.004) for CCL26, -0.343 (*p*=0.006) for CCL13, -0.331 (*p*=0.008) for CCL17, -0.300 (*p*=0.017) for CXCL18, and -0.300 (*p*=0.017) for CXCL1. Given that a slower increase in A β PET SUVR changes is likely indicative of a more favorable prognostic outcome, these findings suggest that higher levels of these chemokines may confer a protective role in recruiting immune cells to attenuate the accumulation of A β plaques. Consistent with this, all five chemokines were lower in abundance in A+ participants, albeit only CCL13 and CCL17 passed the significance cutoff.

We further tested the association of plasma biomarker longitudinal changes with A β PET SUVR changes. Seven NULISaseq targets, namely IL5, p-tau217, A β 38, PGF, CCL2, IL4, and VEGFD, showed strong correlations (Additional file 2: Figure S2). The

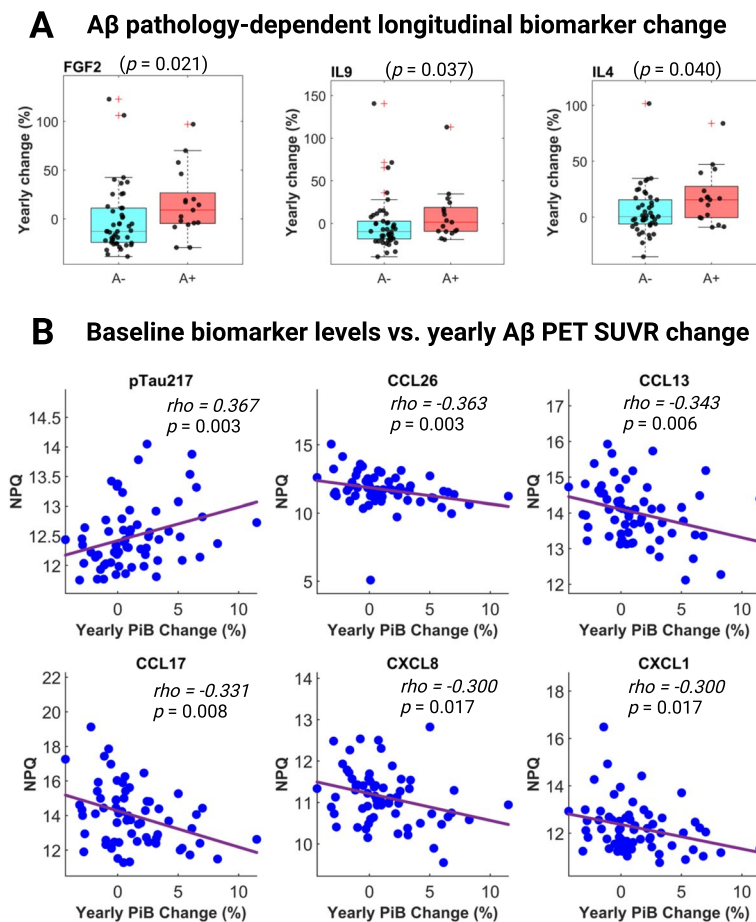
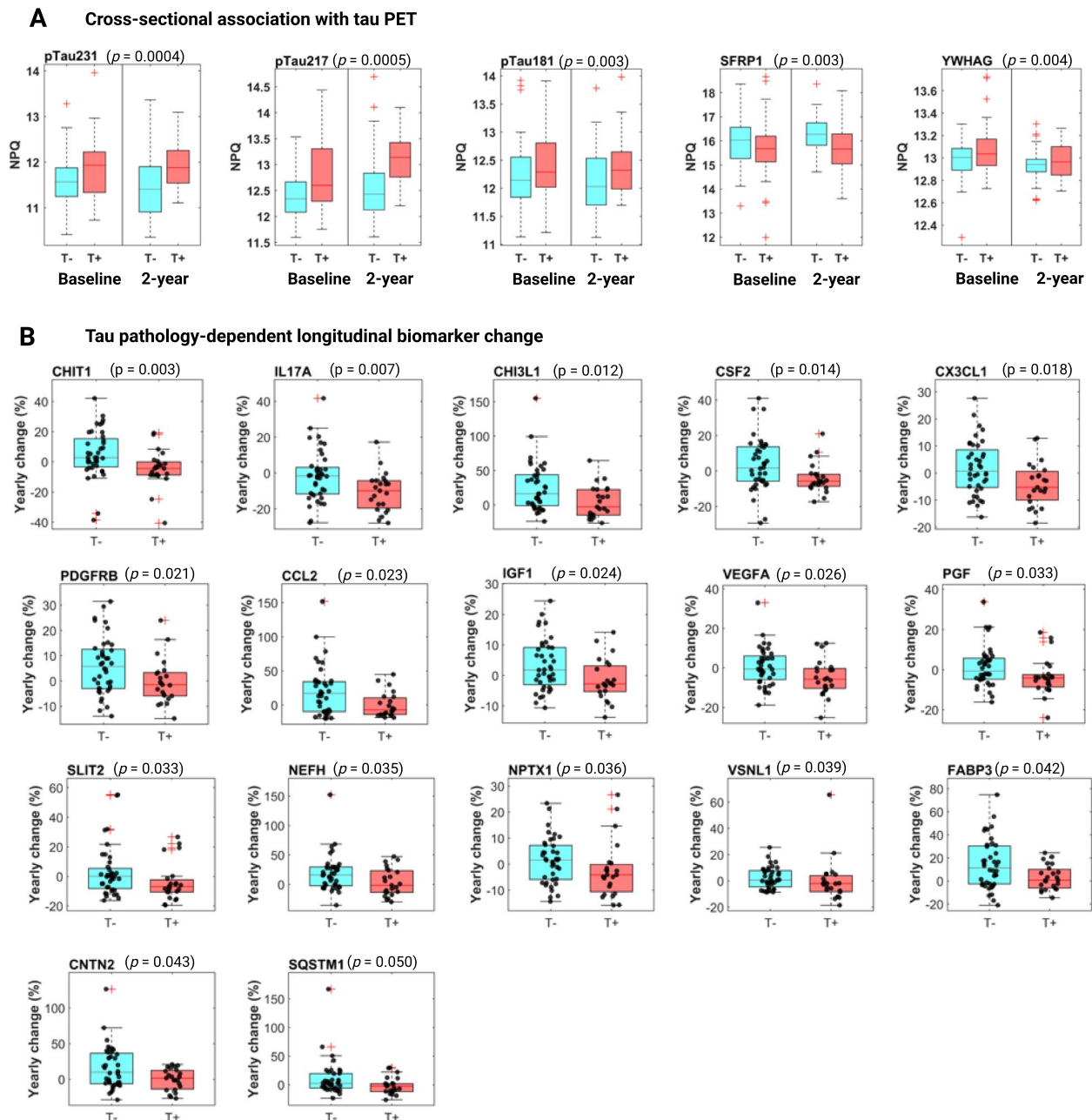


Fig. 3 Longitudinal association between NULISaseq targets and amyloid pathology (A). **A** Boxplots illustrating the distribution of yearly biomarker abundance change by A status. *P*-values were based on two-sided Wilcoxon rank-sum tests. **B** Scatterplots for the correlation between yearly longitudinal A β PET SUVR change and baseline biomarker levels. The strength of the correlation was assessed based on Spearman's ranks. Purple lines indicated the least square regression lines

changes of all seven targets were positively correlated with A β PET SUVR changes, suggesting that upward changes of these targets over time might be correlated with more severe A β pathology.

Association of NULISeq targets with tau pathology (T) Cross-sectional association

Five NULISeq targets displayed significant associations with tau PET positivity according to p -value cutoff of 0.005, corresponding to FDR of 9%, after adjusting for age, sex and APOE ϵ 4 carrier status (Fig. 4A).



The three top significant targets were p-tau species, namely p-tau231 ($p=0.0004$), p-tau217 ($p=0.0005$), and p-tau181 ($p=0.003$). Secreted frizzled-related protein 1 (SFRP1), a Wnt signaling modulator [59], and 14–3-3 protein gamma (YWHAG) were the other significant targets, with p -values of 0.003 and 0.004, respectively. All except SFRP1 were increased in T+ participants. Average fold increases of 29%, 36%, 20%, and 5% in T+ participants compared with T- controls were observed for p-tau231, p-tau217, p-tau181, and YWHAG, respectively. SFRP1, on the other hand, was decreased at an average of 27%. Among these five targets, p-tau217 had the highest diagnostic accuracy in detecting abnormal tau pathology, with AUCs of 0.652 (95% CI: 0.518–0.765) for the baseline cohort and 0.797 (95% CI: 0.660–0.888) for the 2-year cohort. This was followed by p-tau231, which had AUCs of 0.651 (95% CI: 0.522–0.759) and 0.705 (95% CI: 0.560–0.816), respectively. The inclusion of age, sex, and APOE $\epsilon 4$ carrier status only slightly improved the AUCs (Additional file 2: Figure S3). Both p-tau217 and p-tau231 showed better diagnostic accuracies in the 2-year cohort, consistent with the expectation that tau pathology worsens over time and that agreement between the plasma and neuroimaging biomarkers improves with disease progression.

As indicated in Table 1, there was a higher proportion of A+ individuals among those who were T+. To test whether the A β PET status contributed to the observed association between these significant targets and tau PET status, we evaluated the association by including A β PET status in the linear mixed models. All remained significant except for p-tau217, which was trending towards significance ($p=0.068$) after adjusting for the effect of A β PET status. The p -values after adjusting for A β PET status were 0.005, 0.003, 0.005, and 0.001 for p-tau231, p-tau181, SFRP1, and YWHAG, respectively.

Longitudinal association

A total of 17 targets displayed significant tau pathology-dependent longitudinal changes according to the Wilcoxon rank-sum p -value < 0.05 (Fig. 4B). Chitotriosidase-1 (CHIT1), a known indicator of microglial activation [60, 61], emerged as the top significant target ($p=0.003$). Its levels showed slight increases in T- participants, with a median yearly change of 2.7%. T+ participants, on the contrary, exhibited a median yearly decrease of 4.4%. Similarly, CHI3L1 (YKL-40), a biomarker for reactive astrogliosis, also exhibited an increase (median yearly change of 16.3%) in T- participants but a decrease in T+ individuals (median yearly change of -2.8%).

PGF, PDGFRB, and VEGFA, important players in maintaining cerebrovascular integrity, also showed

tau pathology-dependent longitudinal changes. All three exhibited a declining trend over time in T+ participants (median yearly change: PGF, -4.1%; PDGFRB, -1.5%; VEGFA, -5.7%), contrasting with either stable or increased levels observed in T- individuals (median yearly change: PGF, -0.6%; PDGFRB, 5.8%; VEGFA, -0.6%). These findings suggest that tau pathology may be linked to the deterioration of vascular structure. NPTX1, a biomarker of excitatory synaptic pathology, similarly displayed a decreasing trend in T+ participants (median -4.1%/year), in contrast to a slight upward change in T- controls (median 1.6%/year). Additional targets with tau pathology-dependent longitudinal changes included four cytokines (CCL2, CSF2, IL17A, and CX3CL1), proteins involved in synaptic and neuronal dysfunction (VSNL1, CNTN2, and FABP3), IGF1, SLIT2, NEFH, and SQSTM1.

Baseline levels of three NULISaseq targets, interleukin-12 (IL12p70), interferon gamma (IFNG), and RuvB-like 2 (RUVBL2), were significantly associated with tau PET changes between the two visits (Additional file 2: Figure S4A). High baseline levels of IL12p70 and IFNG, two presumptive pro-inflammatory cytokines, were associated with faster progression of tau pathology, as determined by a more pronounced increase in tau PET composite, with ρ of 0.288 ($p=0.022$) and 0.269 ($p=0.033$), respectively. The opposite relationship was recorded for RUVBL2, an AAA-type ATPase involved in regulating pro-inflammatory response. A higher baseline level of RUVBL2 was associated with a smaller increase in tau pathology, with a ρ of -0.253 ($p=0.046$).

The longitudinal change of seven NULISaseq targets correlated significantly with tau PET SUVR change (Additional file 2: Figure S4B). Interestingly, the list included three tau targets, all of which showed positive associations, namely MAPT (t-tau; $\rho=0.348$; $p=0.005$), p-tau217 ($\rho=0.293$; $p=0.020$) and p-tau181 ($\rho=0.251$; $p=0.047$). Other targets on the list included SOD1 ($\rho=0.359$; $p=0.004$), interleukin-6 receptor subunit alpha (IL6R; $\rho=0.292$; $p=0.020$), granulocyte-macrophage colony-stimulating factor (CSF2; $\rho=0.280$; $p=0.027$), and CD40 ligand (CD40LG; $\rho=-0.262$; $p=0.038$).

Association of NULISaseq targets with neurodegeneration (N)

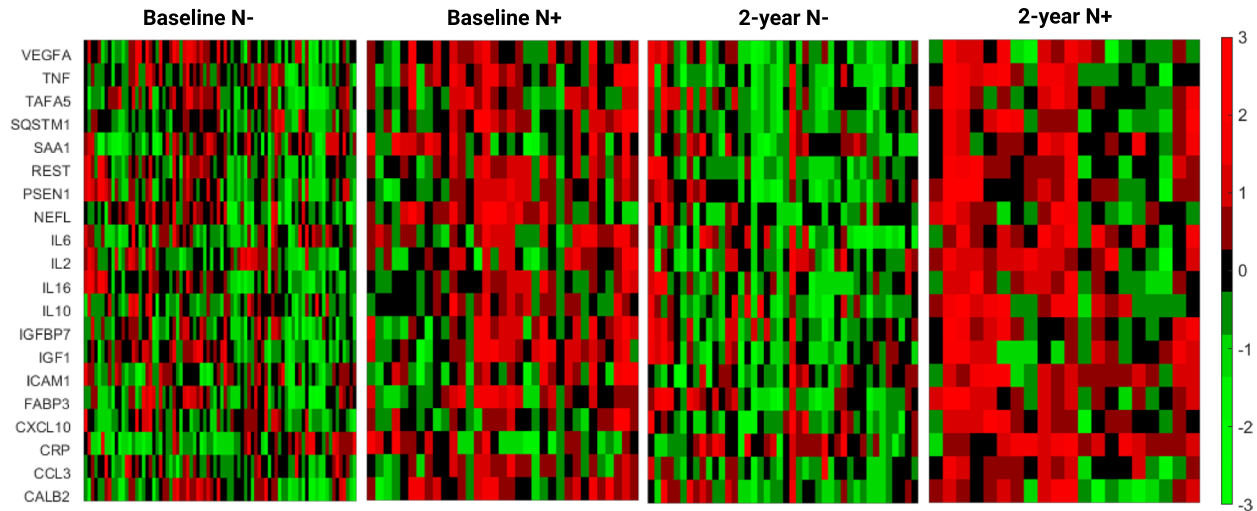
Cross-sectional association

Twenty NULISaseq targets exhibited significant associations with N status when assessed using univariate analysis with dichotomous outcomes (N- vs. N+) or Spearman correlations with MRI-determined cortical thickness (p -value < 0.005 , corresponding to ~5% FDR) without adjusting for the effects of common risk factors. The list of significant targets included NEFL,

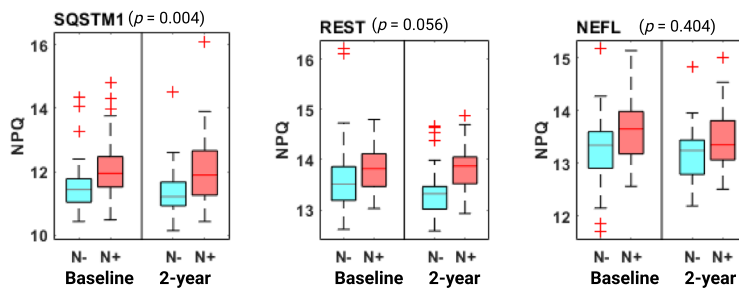
a classical biomarker for neurodegeneration, eight cytokines (IL2, IL6, IL10, IL16, TNF, CCL3, CXCL10, and TFA5), proteins previously linked to synaptic and neuronal network defects (CALB2, FABP3, and REST), proteins involved in regulating proteostasis (PSEN1, and SQSTM1), proteins involved in acute-phase

response (CRP, SAA1 and SAA2), and ICAM1 and VEGFA, both critical for maintaining cerebrovascular integrity. As depicted in the heatmap in Fig. 5A, these targets exhibited a consistent trend in both the baseline and 2-year visit samples, with all targets upregulated in N+ individuals compared with N- controls.

A NULISaseq targets exhibiting significant univariate association with N status



B Boxplot distributions by N status for selected NULISaseq targets



C Targets with N status-dependent change

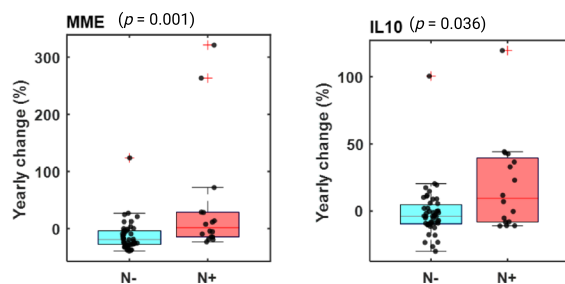


Fig. 5 Association of NULISaseq targets with neurodegeneration (N). **A** Heatmaps illustrating the abundance levels of NULISaseq with significant univariate associations with N status (unadjusted for covariates). The NPQ values were standardized for each protein target using z-scores. **B** Boxplots of selected NULISaseq targets, separated by N status and visit. *P*-values on top of the boxplots were for the whole data combining both visits and were determined using linear mixed models (random intercepts) with NPQs as the dependent variable, visit-specific N status as the independent variables, adjusting for covariates age, sex, and *APOE* ϵ 4 carrier status. **C** Boxplots illustrating the distribution of yearly biomarker abundance change by N status. *P*-values were based on two-sided Wilcoxon rank-sum tests

The repressor element-1 silencing transcription factor (REST), a zinc finger transcription factor with potential neuroprotective function [62], was one of the top significant targets, with p -values of 0.004 and 0.0008 and AUCs of 0.671 (95% CI 0.561–0.769) and 0.766 (95% CI 0.600–0.883) for the baseline and 2-year visit, respectively (Fig. 5B). NEFL showed a strong association in the baseline samples ($p=0.003$) but not in the 2-year visit samples ($p=0.126$) (Fig. 5B).

However, after adjusting for age, sex, and *APOE* $\epsilon 4$ carrier status, the associations weakened for most of these targets, with sequestosome 1 (SQSTM1) being the only target retaining a p -value < 0.005 . SQSTM1 exhibited strong association with N status in both baseline and 2-year cohorts, with Wilcoxon rank-sum p -values of 0.0001 and 0.006, respectively (Fig. 5B). It distinguished N+ from N- participants with accuracies of 0.729 (95% CI 0.606–0.829) at baseline and 0.713 (95% CI 0.548–0.854) at the 2-year visit (Fig. 5B). The inclusion of common risk factors (age, sex, and *APOE* $\epsilon 4$ carrier status) improved the accuracies to 0.776 (95% CI 0.674–0.860) and 0.848 (95% CI 0.703–0.933).

Longitudinal association

Nephrilysin (MME) and interleukin 10 (IL10) demonstrated neurodegeneration-dependent abundance changes, with increases in N+ participants (median change/year: MME, 1.7%; IL10, 9.4%) and decreases in N- individuals (median change/year: MME, 19.2%; IL10, 3.8%) (Fig. 5C).

Baseline levels of five NULISeq targets – KLK6 (kallikrein related peptidase 6), CCL11, AGRN (agrin), tumor necrosis factor (TNF), and PGK1 – were significantly associated with cortical thickness change, all showing positive correlations, suggesting higher levels of these targets may be linked with a slower rate of neurodegeneration (Additional file 2: Figure S5A). The longitudinal change of five targets – PTN, YWHAZ (14–3-3 protein zeta/delta), GOT1 (glutamic-oxaloacetic transaminase 1), NRGN, A β 42, and SNCA (oligomer) – was significantly correlated with cortical thickness change (Additional file 2: Figure S5B). Among them, A β 42 exhibited a positive correlation with cortical thickness change, with ρ of 0.264 ($p=0.037$), suggesting that a decrease in A β 42 levels is associated with more severe neurodegeneration, i.e., a decrease in cortical thickness. Conversely, changes in the other four targets were negatively associated with cortical thickness change, with ρ of -0.335 ($p=0.008$), -0.291 ($p=0.021$), -0.290 ($p=0.022$), -0.284 ($p=0.025$), for PTN, YWHAZ, GOT1, and NRGN, respectively.

Discussion

In this study, we have demonstrated the feasibility of concurrent immunoassay-based analysis of 116 protein markers in blood to provide diagnostic and prognostic information in preclinical AD. Our results identified several novel inflammation, synaptic, and vascular markers in blood significantly associated with brain A β , tau, and neurodegeneration burden at baseline and at the two-year follow-up. These were not limited to markers such as p-tau217, p-tau231, p-tau181, and GFAP, the elevation of which have consistently shown strong associations with brain A β and/or tau load, but included novel protein targets that inform about the disease state of the individual in different pathological stages across the biological AD continuum. Importantly, this is the first time several of these protein targets have shown validated technical and clinical biomarker potential in blood. These included the cerebrovascular markers ICAM1, VCAM1, PDGFRB, PGF, VEGFA, VEGFD, synaptic marker NPTX1, and glial markers CHIT1 and CHI3L1 (YKL-40).

Concurrent measurement of a large number of protein analytes presents technical challenges that most available immunoassay platforms struggle to address. Problems such as reagent cross-activity and the dynamic range of target analyte abundance impede the multiplexing capacity of immunoassays. Technological breakthroughs, including antibody arrays, proximity ligation assay (PLA), proximity extension assay (PEA), microsphere bead capture technology by Luminex, and slow off-rate modified aptamer assay (SOMAscan), have enabled the simultaneous measurement of hundreds to thousands of plasma proteins [63]. Among them, PEA-based Olink and SOMAscan stand out for their multianalyte measurement capacities, capable of measuring thousands of proteins in a single assay. A number of studies have utilized these proteomic platforms for AD biomarker research, leading to the identification of several emerging AD biomarkers and biomarker panels [64–67].

The NULISA technology, which is built as an advancement of the PLA technique, integrates multiple mechanisms to enhance the performance of PLA, including a proprietary sequential immunocomplex capture and release mechanism for background reduction, next-generation sequencing-based signal readout, and fine-tuning the ratio of unconjugated "cold" antibodies to DNA-conjugated "hot" antibodies to mitigate sequencing reads of high-abundant proteins. This provides the proteomic platform the capability to detect hundreds of protein biomarkers with attomolar sensitivity and ultra-broad dynamic range [34]. The high detectability rate and low detection limits for the various protein targets in this study support this. Compared to the highly multiplex Olink and SOMAscan platforms, which are designed to

measure a large number of proteins for discovery applications, the NULISaseq CNS panel offers more targeted measurements of established Alzheimer's Disease biomarkers and emerging biomarkers with known associations with neurodegenerative diseases.

The strong correlation and comparable diagnostic accuracies in the head-to-head comparisons with Simoa assays indicate that both techniques measure equivalent pools of the protein targets available in the blood. It is worth mentioning that the exceptional correlation with the Simoa ALZPath assay could be due to the two assays using the same p-tau217 monoclonal antibody.

The high performance of plasma p-tau217, p-tau231, and GFAP to identify abnormal A β PET scans in this mostly cognitively normal cohort is corroborated by findings from several recent studies based on results from other analytical platforms [9, 68–72]. Importantly, we identified biomarkers with decreased levels in A+ participants, akin to plasma A β 42 and A β 42/40, indicating reduced availability in blood with progressive brain A β pathology. The decreases in TIMP3 are consistent with previously reported lower TIMP3 levels in AD patients [73]. TIMP3 also promotes brain A β production via inhibiting α -secretase cleavage of the amyloid precursor protein [74]. Reduction in MDH1 levels supports previous reports on the involvement of altered energy metabolism in late-onset AD [75, 76] while BDNF has been implicated in a protective role against A β peptides-induced neurotoxicity [77]. Several inflammatory cytokines were among the significantly down-regulated biomarkers, consistent with published literature that linked multiple inflammatory cytokines to A β pathology in AD cases and those resilient to AD [78–80]. FGF2 gene transfer reversed hippocampal function and cognitive decline in mouse models [81]. Similarly, beneficial effects of IL4 have been reported in animal models [81].

Plasma p-tau217, p-tau231, and p-tau181 were the leading markers to identify abnormal tau-PET scans. However, accounting for A β PET status in the combined A and T positivity analysis suggested that the results were partly explained by the strong association of these markers with A β pathology. This could mean that the tau forms containing these phosphorylation sites become available in blood in the early phases of A β plaque pathology. Aside from blood-based tau markers, YWHAG [82–84] and SFRP1 [85] showed strong associations with AD. The reduction in SFRP1 levels might be explained by its direct binding to A β plaques [86]. Importantly, the existing evidence from these markers has been built in CSF and brain tissue samples. Here, we extend these findings to blood.

The reactive astrogliosis marker CHI3L1 (YKL-40) and the microglia activation marker CHIT1 have repeatedly

been shown to be associated with tau pathology; however, the evidence base has only been built using CSF samples [6, 87, 88]. In our study, both proteins exhibited tau pathology-dependent longitudinal changes, increasing in T- participants but decreasing in T+ participants who were also A β -positive. These observations suggest that A β pathology may trigger early activation of the brain's immune system to mitigate damage, but this response may plateau or decrease as more downstream pathology, such as tau pathology, becomes apparent. Alternatively, lower glial activation in response to amyloid and tau pathology may reflect the resilience of pathologically burdened but cognitively preserved individuals [78, 89]. Tau pathology-dependent longitudinal changes were also observed in the vascular markers PGF, PDGFRB, and VEGFA, and the synaptic marker NPTX1. The biomarker potential of all these biomarkers has been demonstrated in CSF [21, 90–96]. Translation of these prior findings to plasma indicates that the molecular processes in AD involving these markers are reflected in the bloodstream, expanding the repertoire of blood-based indicators of brain pathophysiological changes.

Our study identified several plasma biomarkers with strong associations with neurodegeneration assessed based on cortical thickness, including NEFL, which is a proven general marker of neuronal injury [97, 98]. Not surprisingly, several cytokines, including IL2, IL6, IL10, IL16, TNF, CCL3, CXCL10, and TFAA5, also showed significant associations with neurodegeneration, reinforcing the close relationship between neuroinflammation and neurodegenerative processes [99, 100].

Two vascular proteins, ICAM1 and VEGFA, were on the significant list, consistent with the expected involvement of neurovascular dysfunction in neuroinflammation and neurodegeneration [101]. ICAM1 is a transmembrane glycoprotein expressed in multiple cell types and plays a key role in maintaining the blood brain barrier (BBB) [102]. Its expression is induced by neuroinflammation, leading to increased leukocyte transmigration across the BBB, a key event in the pathogenesis of various brain diseases, including AD [103–105]. Consistent with this, our study observed elevated ICAM1 levels in participants with neurodegeneration, aligning with previous research [18, 20]. VEGFs have complex associations with neurological diseases, exhibiting both neuroprotective and neuro-destructive potentials [24, 25, 106]. We observed elevated VEGFA levels in N+ participants and a faster decline in VEGFA levels in T+ participants, suggesting a potential staging effect. Interestingly, a recent study showed that a low level of VEGFA, measured with assays from Meso Scale Discovery, was associated with accelerated neocortical tau accumulation in preclinical A+ participants in the Harvard Aging Brain Study [107].

Synaptic and neuronal network dysfunction, along with aberrant proteostasis, represent two of the eight pathological hallmarks of neurodegenerative diseases [35]. In alignment with this, we found significant associations between neurodegeneration, three synaptic/network proteins (CALB2, FABP3, and REST), and two proteostatic regulators (PSEN1 and SQSTM1). Notably, among all targets with significant association with neurodegeneration, only SQSTM1 withstood corrections for age, sex, and *APOE* ϵ 4 genotype, revealing it as a potentially novel neurodegeneration biomarker for AD, with respect to cortical thickness. SQSTM1, a scaffold protein with a critical role in macroautophagy, has been previously linked to several neurodegenerative diseases, including AD [108–110].

IL10 and MME were the top hits with differential longitudinal changes in N+ vs. N- participants. Several studies support their roles as markers of neurodegeneration status. For example, an animal model study suggested that the mechanisms of action of IL-10 as an inflammatory response might be through the activation of microglia, which leads to IL-6 activation and abnormal phosphorylation of tau [111]. MME is an integral membrane-bound metalloproteinase (MMP) and one of the key enzymes involved in A β degradation [112]. MMPs have been found to exhibit dual roles in AD pathogenesis. On the one hand, they can reduce the amount of A β deposits by degrading A β peptides [113, 114]. On the other hand, their levels can be induced by A β , potentially leading to brain parenchymal destruction [115, 116].

Interestingly, while a number of cytokines (IL2, IL6, IL10, IL16, TNF, CCL3, CXCL10, and TFAF5) were increased in participants with neurodegeneration, several cytokines (IL7, IL13, CD40LG, CCL13, CCL17, and CCL22) were found to be decreased in participants with A β pathology. Additionally, higher baseline levels of several chemokines (CCL26, CCL17, CCL13, CXCL1, and CXCL8) were significantly associated with slower progression of A β pathology. Given that most participants with A β pathology were cognitively normal, and neurodegeneration is presumed to occur at a later stage than the early phase of A β pathology, our results support the biphasic roles of neuroinflammation, with protective effects in the early stages and potentially detrimental effects in the later stages. These findings are in line with the recognized multifaceted impact of neuroinflammation on AD pathogenesis [117, 118].

Our study identified several biomarkers exhibiting pathology-dependent longitudinal changes. Specifically, FGF2, IL4, and IL9 showed A β pathology-dependent changes; several biomarkers associated with neuroinflammation, synaptic function, and cerebrovascular integrity demonstrated tau pathology-dependent changes; and

MME and IL10 exhibited neurodegeneration-dependent changes. These findings may enhance our understanding of the natural history of AD, allowing for better staging of the disease. They can also aid in its diagnosis and prognosis, guide the development of therapeutic interventions to slow disease progression, and monitor the efficacy of treatments.

Strengths of this study include (i) technical validation of the new NULISA platform; (ii) direct comparison of the clinical performances of biomarkers measured using NULISA assays vs. with Simoa assays; (iii) focus on a population-based cohort to provide information closer to the real world than most clinical research-based cohorts; (iv) emphasis on predominantly cognitively normal participants with emerging pathological phenotypes, to test the sensitivity of the NULISA platform to these incipient changes; (v) availability of paired neuroimaging measures of A β , tau, and neurodegeneration, making it possible to identify inflammatory, vascular and synaptic markers associated with abnormal changes in different biologically defined disease stages; and (vi) repeated neuroimaging evaluations and blood collection over a two-year interval, allowing to examine biomarker changes within that timeframe.

Limitations include the lack of validation in larger and more diverse cohorts. Our cohort primarily consists of mostly non-Hispanic White participants, despite being representative of the catchment area. More diverse cohorts will be needed to determine whether our findings are transferable to the general population. Additionally, since the majority of participants were cognitively normal at both visits, our study does not allow for the examination of the association between NULISAseq biomarkers and cognitive function throughout the disease continuum. Lifestyle factors and comorbidities can significantly influence blood biomarkers, as recognized by recent review papers [119, 120]. However, due to the small sample size, we could not incorporate their impact into our analysis. Furthermore, the significance of longitudinal changes was based on short-term follow-up. Cohorts with longer-term follow-up, particularly those tracking clinical outcomes such as cognitive decline and the progression of AD pathology, are needed to further evaluate the clinical utility of these biomarkers.

Conclusions

Together, this targeted proteomic study has established that results from the NULISA platform are equivalent to those from Simoa HDX. Additionally, the strong multiplexing capabilities of NULISA allowed for the evaluation of dozens of verified and putative protein biomarkers in a longitudinal preclinical AD cohort. We identified several neuroinflammation, synaptic, and vascular markers that

have been previously linked to AD, but their measurement in plasma was hitherto not established. Our findings, therefore, pave the way for independent validation of these plasma markers to enable their widespread use for diagnostic, prognostic, and monitoring.

Abbreviations

A β	Amyloid-beta
AD	Alzheimer's disease
ANXA5	Annexin A5
AGRN	Agrin
AUC	Area under Curve
BBB	Blood brain barrier
CD40LG	CD40 ligand
CDR	Clinical dementia rating
CHI3L1	Chitinase-3 like-protein-1
CHIT1	Chitotriosidase-1
CNS	Central nervous system
CNTN2	Contactin 2
CSF	Cerebrospinal fluid
CSF2	Granulocyte-macrophage colony-stimulating factor
CV	Coefficient of variation
FDR	False discovery rate
GOT1	Glutamic-oxaloacetic transaminase 1
IC	Internal control
ICAM1	Intercellular adhesion molecule 1
IFNG	Interferon gamma
IL10	Interleukin 10
IL12p70	Interleukin-12 (IL12p70)
IL6R	Interleukin-6 receptor subunit alpha
IQR	Interquartile range
IPC	Inter-plate control
KLK6	Kallikrein related peptidase 6
LOD	Limit of detection
MCI	Mild cognitive impairment
MDH1	Malate dehydrogenase subunit 1
MME	Nephrilysin
MMSE	Mini-Mental State Examination
MRI	Magnetic resonance imaging
MYHAT	Monongahela Youghioghenny Healthy Aging Team
MYHAT -NI	Monongahela Youghioghenny Healthy Aging Team-Neuroimaging
NEFH	Neurofilament heavy chain
NEFL	Neurofilament light chain
NPQ	NULISA protein quantification
NPTX1	Neuronal pentraxin-1
NRGN	Neurogranin
NULISA	NUcleic acid-linked Immuno-Sandwich Assay
NULISAseq	NULISA with next-generation sequencing readout
OligoSNCA	Oligomeric α -synuclein
PEA	Proximity extension assay
PET	Positron emission tomography
PiB	Pittsburgh compound-B
PDGFRB	Soluble platelet-derived growth factor receptor β
PGK1	Phosphoglycerate kinase 1
PLA	Proximity ligation assay
p-tau	Phosphorylated tau
pTDP43-409	TDP43 phosphorylated at Ser409
PTN	Pleiotrophin
QC	Quality control
ROC	Receiver operating characteristic
ROIs	Regions of interest
RUVBL2	RuvB-like 2
SD	Standard deviation
SFRP1	Secreted frizzled-related protein 1
Simoa	Single-molecule array
SNCA	α -Synuclein
SOD1	Superoxide dismutase 1
SQSTM1	Sequestosome 1
SUVR	Standardized uptake value ratio

TIMP3	Metalloproteinase inhibitor 3
TNF	Tumor necrosis factor
UCHL1	Ubiquitin C-terminal hydrolase L1
VCAM1	Vascular cell adhesion molecule 1
VEGF	Vascular endothelial growth factor
YWHAG	14-3-3 Protein gamma
YWHAZ	14-3-3 Protein zeta/delta

Supplementary Information

The online version contains supplementary material available at <https://doi.org/10.1186/s13024-024-00753-5>.

Additional file 1: List of biomarkers included in the NULISAseq CNS panel.

Additional file 2: Supplementary Figure S1 to S5.

Acknowledgements

We thank all members of the Karikari Laboratory for their support and Dr. Rebecca Deek for statistical advice. We are indebted to the participants, family members, and staff of the MYHAT-NI study.

Authors' contributions

TKK, MIK, ADC, BES, and MG contributed to the study's conception and design. BES and MG ran MYHAT and MYHAT-NI cohorts. ADC, VLV, TAP, PCLF, BB, GP, OIL and WEK contributed to neuroimaging data collection and analysis. TKL, AS, PCF, BB, and PG performed biochemical assays. MIK performed genotyping experiments. XZ and YC performed data analysis and produced the figures. XZ and TKK were major contributors in writing the manuscript. All authors contributed to and approved the final version of the manuscript.

Funding

The MYHAT study was supported by R37 AG023651-17 and MYHAT-NI by R01 AG052521. TKK and the Karikari Laboratory were supported by the NIH (R01 AG083874, U24 AG082930, P30 AG066468, RF1 AG052525-01A1, R01 AG053952-05, R37 AG023651-17, RF1 AG025516-12A1, R01 AG073267-02, R01 AG075336-01, R01 AG072641-02, P01 AG025204-16) and the Alzheimer's Association (#AARF-21-850325). MDI was supported by NIH/NIA grants P01AG14449 and P01AG025204.

Availability of data and materials

De-identified, cohort-level data will be shared at the request of verified investigators to replicate procedures and results reported in this article. Data transfer agreements in accordance with US legislation and the decisions of the University of Pittsburgh's Institutional Review Board, which covers the jurisdiction of the MYHAT-NI study, may need to be established.

Declarations

Ethics approval and consent to participate

All plasma samples were obtained with full written informed consent and approved by the University of Pittsburgh Institutional Review Board (STUDY19020264).

Consent for publication

Not applicable.

Competing interests

Dr. Karikari has served as a consultant to Quanterix Corp., unrelated to the submitted work. The other authors declare that they have no competing interests.

Author details

¹Department of Psychiatry, School of Medicine, University of Pittsburgh, 3811 O'Hara Street, Pittsburgh, PA 15213, USA. ²Department of Chemistry, University of Pittsburgh, Pittsburgh, PA 15213, USA. ³Department of Human Genetics, School of Public Health, University of Pittsburgh, Pittsburgh, PA 15213, USA. ⁴Department of Neurology, School of Medicine, University of Pittsburgh, Pittsburgh, PA 15213, USA. ⁵Geriatric Research Education and Clinical Center, VA Pittsburgh HS, Pittsburgh, PA, USA. ⁶Department of Epidemiology, School of Public Health, University of Pittsburgh, Pittsburgh, PA, USA.

Received: 23 April 2024 Accepted: 4 September 2024
Published online: 10 October 2024

References

- Jack Jr. CR, Andrews JS, Beach TG, Buracchio T, Dunn B, Graf A, Hansson O, Ho C, Jagust W, McDade E, et al. Revised criteria for diagnosis and staging of Alzheimer's disease: Alzheimer's Association Workgroup. *Alzheimers Dement*. 2024;20:5143–69.
- Jack CR, Bennett DA, Blennow K, Carrillo MC, Dunn B, Haeberlein SB, Holtzman DM, Jagust W, Jessen F, Karlawish J, et al. NIA-AA research framework: toward a biological definition of Alzheimer's disease. *Alzheimers Dement*. 2018;14:535–62.
- Selkoe DJ. Alzheimer's disease is a synaptic failure. *Science*. 2002;298:789–91.
- Maslah E. Mechanisms of synaptic dysfunction in Alzheimer's disease. *Histol Histopathol*. 1995;10:509–19.
- Lleó A, Núñez-Llaves R, Alcolea D, Chiva C, Balateu-Pañós D, Colom-Cadena M, Gomez-Giro G, Muñoz L, Querol-Vilaseca M, Pegueroles J, et al. Changes in synaptic proteins precede neurodegeneration markers in preclinical Alzheimer's disease cerebrospinal fluid. *Mol Cell Proteomics*. 2019;18:546–60.
- Ferrari-Souza JP, Ferreira PCL, Bellaver B, Tissot C, Wang Y-T, Leffa DT, Brum WS, Benedet AL, Ashton NJ, De Bastiani MA, et al. Astrocyte biomarker signatures of amyloid- β and tau pathologies in Alzheimer's disease. *Mol Psychiatry*. 2022;27:4781–9.
- Pelkmans W, Shekari M, Brugulat-Serrat A, Sánchez-Benavides G, Minguilón C, Fauria K, Molinuevo JL, Grau-Rivera O, González Escalante A, Kollmorgen G, et al. Astrocyte biomarkers GFAP and YKL-40 mediate early Alzheimer's disease progression. *Alzheimers Dement*. 2024;20:483–93.
- Antonell A, Mansilla A, Rami L, Lladó A, Iranzo A, Olives J, Balasa M, Sánchez-Valle R, Molinuevo JL. Cerebrospinal fluid level of YKL-40 protein in preclinical and prodromal Alzheimer's disease. *J Alzheimers Dis*. 2014;42:901–8.
- Pereira JB, Janelidze S, Smith R, Mattsson-Carlsson N, Palmqvist S, Teunissen CE, Zetterberg H, Stomrud E, Ashton NJ, Blennow K, Hansson O. Plasma GFAP is an early marker of amyloid- β but not tau pathology in Alzheimer's disease. *Brain*. 2021;144:3505–16.
- Suárez-Calvet M, Morenas-Rodríguez E, Kleinberger G, Schlepckow K, Araque Caballero MÁ, Franzmeier N, Capell A, Fellerer K, Nuscher B, Eren E, et al. Early increase of CSF sTREM2 in Alzheimer's disease is associated with tau related-neurodegeneration but not with amyloid- β pathology. *Mol Neurodegener*. 2019;14:1.
- Park S-H, Lee E-H, Kim H-J, Jo S, Lee S, Seo SW, Park H-H, Koh S-H, Lee J-H. The relationship of soluble TREM2 to other biomarkers of sporadic Alzheimer's disease. *Sci Rep*. 2021;11:13050.
- Rauchmann B-S, Schneider-Axmann T, Alexopoulos P, Perneczky R. CSF soluble TREM2 as a measure of immune response along the Alzheimer's disease continuum. *Neurobiol Aging*. 2019;74:182–90.
- Heslegrave A, Heywood W, Paterson R, Magdalinos N, Svensson J, Johansson P, Öhrfelt A, Blennow K, Hardy J, Schott J, et al. Increased cerebrospinal fluid soluble TREM2 concentration in Alzheimer's disease. *Mol Neurodegener*. 2016;11:3.
- Hok AHYS, Del Campo M, Boiten WA, Stoops E, Vanhooren M, Lemstra AW, van der Flier WM, Teunissen CE. Neuroinflammatory CSF biomarkers MIF, sTREM1, and sTREM2 show dynamic expression profiles in Alzheimer's disease. *J Neuroinflammation*. 2023;20:107.
- Motta C, Finardi A, Toniolo S, Di Lorenzo F, Scaramazza E, Loizzo S, Mercuri NB, Furlan R, Koch G, Martorana A. Protective role of cerebrospinal fluid inflammatory cytokines in patients with amnesic mild cognitive impairment and early Alzheimer's disease carrying apolipoprotein E4 genotype. *J Alzheimers Dis*. 2020;76:681–9.
- Doroszkiwicz J, Kulczyńska-Przybik A, Dulewicz M, Borawska R, Krawiec A, Slowik A, Mroczko B. The cerebrospinal fluid interleukin 8 (IL-8) concentration in Alzheimer's disease (AD). *Alzheimers Dement*. 2021;17:e051317.
- Taipia R, das Neves SP, Sousa AL, Fernandes J, Pinto C, Correia AP, Santos E, Pinto PS, Carneiro P, Costa P, et al. Proinflammatory and anti-inflammatory cytokines in the CSF of patients with Alzheimer's disease and their correlation with cognitive decline. *Neurobiol Aging*. 2019;76:125–32.
- Janelidze S, Mattsson N, Stomrud E, Lindberg O, Palmqvist S, Zetterberg H, Blennow K, Hansson O. CSF biomarkers of neuroinflammation and cerebrovascular dysfunction in early Alzheimer disease. *Neurology*. 2018;91:e867–77.
- Bettcher BM, Johnson SC, Fitch R, Casaleto KB, Heffernan KS, Asthana S, Zetterberg H, Blennow K, Carlsson CM, Neuhaus J, et al. Cerebrospinal fluid and plasma levels of inflammation differentially relate to CNS markers of Alzheimer's disease pathology and neuronal damage. *J Alzheimers Dis*. 2018;62:385–97.
- Rauchmann B-S, Sadlon A, Perneczky R, for the Alzheimer's Disease Neuroimaging I. Soluble TREM2 and inflammatory proteins in Alzheimer's disease cerebrospinal fluid. *J Alzheimers Dis*. 2020;73:1615–26.
- Miners JS, Kehoe PG, Love S, Zetterberg H, Blennow K. CSF evidence of pericyte damage in Alzheimer's disease is associated with markers of blood-brain barrier dysfunction and disease pathology. *Alzheimer's Res Ther*. 2019;11:81.
- Wang J, Fan D-Y, Li H-Y, He C-Y, Shen Y-Y, Zeng G-H, Chen D-W, Yi X, Ma Y-H, Yu J-T, Wang Y-J. Dynamic changes of CSF sPDGFR β during ageing and AD progression and associations with CSF ATN biomarkers. *Mol Neurodegener*. 2022;17:9.
- Lv X, Zhang M, Cheng Z, Wang Q, Wang P, Xie Q, Ni M, Shen Y, Tang Q, Gao F, China Aging Neurodegenerative Disorder Initiative C. Changes in CSF sPDGFR β level and their association with blood-brain barrier breakdown in Alzheimer's disease with or without small cerebrovascular lesions. *Alzheimer's Res Ther*. 2023;15:51.
- Storkebaum E, Carmeliet P. VEGF: a critical player in neurodegeneration. *J Clin Invest*. 2004;113:14–8.
- Garcia KO, Ornellas FL, Martin PK, Patti CL, Mello LE, Frussa-Filho R, Han SW, Longo BM. Therapeutic effects of the transplantation of VEGF over-expressing bone marrow mesenchymal stem cells in the hippocampus of murine model of Alzheimer's disease. *Front Aging Neurosci*. 2014;6:30.
- Galasko D, Xiao M, Xu D, Smirnov D, Salmon DP, Dewit N, Vanbrabant J, Jacobs D, Vanderstichele H, Vanmechelen E, et al. Synaptic biomarkers in CSF aid in diagnosis, correlate with cognition and predict progression in MCI and Alzheimer's disease. *Alzheimer's & Dement Transl Res Clin Intervent*. 2019;5:871–82.
- Dulewicz M, Kulczyńska-Przybik A, Slowik A, Borawska R, Mroczko B. Neurogranin and neuronal pentraxin receptor as synaptic dysfunction biomarkers in Alzheimer's disease. *J Clin Med*. 2021;10:4575.
- Libiger O, Shaw LM, Watson MH, Nairn AC, Umaña KL, Biarnes MC, Canet-Avilés RM, Jack CR Jr, Breton Y-A, Cortes L, et al. Longitudinal CSF proteomics identifies NPTX2 as a prognostic biomarker of Alzheimer's disease. *Alzheimers Dement*. 2021;17:1976–87.
- Pilotto A, Bongianini M, Tirloni C, Galli A, Padovani A, Zanuso G. CSF alpha-synuclein aggregates by seed amplification and clinical presentation of AD. *Alzheimers Dement*. 2023;19:3754–9.
- Anderson NL, Anderson NG. The human plasma proteome: history, character, and diagnostic prospects*. *Mol Cell Proteomics*. 2002;1:845–67.
- Galasko D, Golde TE. Biomarkers for Alzheimer's disease in plasma, serum and blood - conceptual and practical problems. *Alzheimer's Res Ther*. 2013;5:10.
- Kvartsberg H, Portelius E, Andreasson U, Brinkmalm G, Hellwig K, Lelental N, Kornhuber J, Hansson O, Minthon L, Spitzer P, et al. Characterization of the postsynaptic protein neurogranin in paired cerebrospinal fluid and plasma samples from Alzheimer's disease patients and healthy controls. *Alzheimers Res Ther*. 2015;7:40.
- De Vos A, Jacobs D, Struyfs H, Franssen E, Andersson K, Portelius E, Andreasson U, De Surlon D, Hernalsteen D, Sleegers K, et al. C-terminal neurogranin is increased in cerebrospinal fluid but unchanged in plasma in Alzheimer's disease. *Alzheimers Dement*. 2015;11:1461–9.
- Feng W, Beer JC, Hao Q, Ariyapala IS, Sahajan A, Komarov A, Cha K, Moua M, Qiu X, Xu X, et al. NULISA: a proteomic liquid biopsy platform with attomolar sensitivity and high multiplexing. *Nat Commun*. 2023;14:7238.
- Wilson DM 3rd, Cookson MR, Van Den Bosch L, Zetterberg H, Holtzman DM, Dewachter I. Hallmarks of neurodegenerative diseases. *Cell*. 2023;186:693–714.

36. Sullivan KJ, Liu A, Chang CH, Cohen AD, Lopresti BJ, Minhas DS, Laymon CM, Klunk WE, Aizenstein H, Nadkarni NK, et al. Alzheimer's disease pathology in a community-based sample of older adults without dementia: The MYHAT neuroimaging study. *Brain Imaging Behav.* 2021;15:1355–63.
37. Ganguli M, Fu B, Snitz BE, Hughes TF, Chang CC. Mild cognitive impairment: incidence and vascular risk factors in a population-based cohort. *Neurology.* 2013;80:2112–20.
38. Ganguli M, Chang CC, Snitz BE, Saxton JA, Vanderbilt J, Lee CW. Prevalence of mild cognitive impairment by multiple classifications: The Monongahela-Youghiohgheny Healthy Aging Team (MYHAT) project. *Am J Geriatr Psychiatry.* 2010;18:674–83.
39. Morris JC. The Clinical Dementia Rating (CDR): current version and scoring rules. *Neurology.* 1993;43:2412–4.
40. Zeng X, Chen Y, Sehrawat A, Lee J, Lafferty TK, Kofler J, Berman SB, Sweet RA, Tudorascu DL, Klunk WE, et al. Alzheimer blood biomarkers: practical guidelines for study design, sample collection, processing, biobanking, measurement and result reporting. *Mol Neurodegener.* 2024;19:40.
41. Klunk WE, Engler H, Nordberg A, Wang Y, Blomqvist G, Holt DP, Bergström M, Savitcheva I, Huang GF, Estrada S, et al. Imaging brain amyloid in Alzheimer's disease with Pittsburgh Compound-B. *Ann Neurol.* 2004;55:306–19.
42. Lois C, Gonzalez I, Johnson KA, Price JC. PET imaging of tau protein targets: a methodology perspective. *Brain Imaging Behav.* 2019;13:333–44.
43. Kamboh MI, Fan KH, Yan Q, Beer JC, Snitz BE, Wang X, Chang CH, Demirci FY, Feingold E, Ganguli M. Population-based genome-wide association study of cognitive decline in older adults free of dementia: identification of a novel locus for the attention domain. *Neurobiol Aging.* 2019;84:239.e215–239.e224.
44. Lopez OL, Becker JT, Chang Y, Klunk WE, Mathis C, Price J, Aizenstein HJ, Snitz B, Cohen AD, DeKosky ST, et al. Amyloid deposition and brain structure as long-term predictors of MCI, dementia, and mortality. *Neurology.* 2018;90:e1920–8.
45. Snitz BE, Tudorascu DL, Yu Z, Campbell E, Lopresti BJ, Laymon CM, Minhas DS, Nadkarni NK, Aizenstein HJ, Klunk WE, et al. Associations between NIH toolbox cognition battery and in vivo brain amyloid and tau pathology in non-demented older adults. *Alzheimers Dement (Amst).* 2020;12:e12018.
46. Baker SL, Maass A, Jagust WJ. Considerations and code for partial volume correcting [(18)F]-AV-1451 tau PET data. *Data Brief.* 2017;15:648–57.
47. Maass A, Landau S, Baker SL, Horng A, Lockhart SN, La Joie R, Rabinovici GD, Jagust WJ. Comparison of multiple tau-PET measures as biomarkers in aging and Alzheimer's disease. *Neuroimage.* 2017;157:448–63.
48. Gogola A, Lopresti BJ, Tudorascu D, Snitz B, Minhas D, Doré V, Ikonomic MD, Shaaban CE, Matan C, Bourgeat P, et al. Biostatistical Estimation of Tau Threshold Hallmarks (BETH) algorithm for human tau PET imaging studies. *J Nucl Med* 2023;64(11):1798–805.
49. Jack CR Jr, Wiste HJ, Weigand SD, Therneau TM, Lowe VJ, Knopman DS, Gunter JL, Senjem ML, Jones DT, Kantarci K, et al. Defining imaging biomarker cut points for brain aging and Alzheimer's disease. *Alzheimers Dement.* 2017;13:205–16.
50. Benjamini Y, Hochberg Y. Controlling the false discovery rate: a practical and powerful approach to multiple testing. *J Roy Stat Soc: Ser B (Methodol).* 1995;57:289–300.
51. DeLong ER, DeLong DM, Clarke-Pearson DL. Comparing the areas under two or more correlated receiver operating characteristic curves: a nonparametric approach. *Biometrics.* 1988;44:837–45.
52. Robin X, Turck N, Hainard A, Tiberti N, Lisacek F, Sanchez J-C, Müller M. pROC: an open-source package for R and S+ to analyze and compare ROC curves. *BMC Bioinformatics.* 2011;12:77.
53. Goedhart J, Luijsterburg MS. VolcanoNoseR is a web app for creating, exploring, labeling and sharing volcano plots. *Sci Rep.* 2020;10:20560.
54. Kind AJH, Buckingham WR. Making neighborhood-disadvantage metrics accessible - the neighborhood atlas. *N Engl J Med.* 2018;378:2456–8.
55. Uhlen M, Karlsson MJ, Zhong W, Tebani A, Pou C, Mikes J, Lakshminanth T, Forsström B, Edfors F, Odeberg J, et al. A genome-wide transcriptomic analysis of protein-coding genes in human blood cells. *Science* 2019;366(6472):eaax9198.
56. Uhlen M, Karlsson MJ, Hober A, Svensson AS, Scheffel J, Kotol D, Zhong W, Tebani A, Strandberg L, Edfors F, et al. The human secretome. *Sci Signal* 2019;12(609):eaaz0274.
57. Apte SS, Olsen BR, Murphy G. The gene structure of tissue inhibitor of metalloproteinases (TIMP)-3 and its inhibitory activities define the distinct TIMP gene family. *J Biol Chem.* 1995;270:14313–8.
58. Costa S, Ragusa MA, Lo Buglio G, Scilabra SD, Nicosia A. The repertoire of tissue inhibitors of metalloproteinases: evolution, regulation of extracellular matrix proteolysis. *Eng Ther Challenges Life.* 2022;12:1145.
59. Uren A, Reichsman F, Anest V, Taylor WG, Muraiso K, Bottaro DP, Cumberledge S, Rubin JS. Secreted frizzled-related protein-1 binds directly to Wingless and is a biphasic modulator of Wnt signaling. *J Biol Chem.* 2000;275:4374–82.
60. Steinacker P, Verde F, Fang L, Feneberg E, Oeckl P, Roeber S, Anderl-Straub S, Danek A, Diehl-Schmid J, Fassbender K, et al. Chitotriosidase (CHIT1) is increased in microglia and macrophages in spinal cord of amyotrophic lateral sclerosis and cerebrospinal fluid levels correlate with disease severity and progression. *J Neurol Neurosurg Psychiatry.* 2018;89:239–47.
61. Varghese AM, Ghosh M, Bhagat SK, Vijayalakshmi K, Preethish-Kumar V, Vengalil S, Chevula PCR, Nashi S, Polavarapu K, Sharma M, et al. Chitotriosidase, a biomarker of amyotrophic lateral sclerosis, accentuates neurodegeneration in spinal motor neurons through neuroinflammation. *J Neuroinflamm.* 2020;17:232.
62. Hwang JY, Zukin RS. REST, a master transcriptional regulator in neurodegenerative disease. *Curr Opin Neurobiol.* 2018;48:193–200.
63. Ren AH, Diamandis EP, Kulasingam V. Uncovering the depths of the human proteome: antibody-based technologies for ultrasensitive multiplexed protein detection and quantification. *Mol Cell Proteomics.* 2021;20:100155.
64. Dammer EB, Ping L, Duong DM, Modeste ES, Seyfried NT, Lah JJ, Levey AI, Johnson ECB. Multi-platform proteomic analysis of Alzheimer's disease cerebrospinal fluid and plasma reveals network biomarkers associated with proteostasis and the matrisome. *Alzheimer's Res Ther.* 2022;14:174.
65. Chen J, Doyle MF, Fang Y, Mez J, Crane PK, Scollard P, Satizabal CL, Alosco ML, Qiu WQ, Murabito JM, Lunetta KL. Peripheral inflammatory biomarkers are associated with cognitive function and dementia: Framingham Heart study offspring cohort. *Aging Cell.* 2023;22:e13955.
66. Jiang Y, Zhou X, Ip FC, Chan P, Chen Y, Lai NCH, Cheung K, Lo RMN, Tong EPS, Wong BWY, et al. Large-scale plasma proteomic profiling identifies a high-performance biomarker panel for Alzheimer's disease screening and staging. *Alzheimers Dement.* 2022;18:88–102.
67. Guo Y, You J, Zhang Y, Liu WS, Huang YY, Zhang YR, Zhang W, Dong Q, Feng JF, Cheng W, Yu JT. Plasma proteomic profiles predict future dementia in healthy adults. *Nat Aging.* 2024;4:247–60.
68. Ashton NJ, Brum WS, Di Molfetta G, Benedet AL, Arslan B, Jonaitis E, Langhough RE, Cody K, Wilson R, Carlsson CM, et al. Diagnostic accuracy of a plasma phosphorylated tau 217 immunoassay for Alzheimer Disease pathology. *JAMA Neurol.* 2024;81:255–63.
69. Triana-Baltzer G, Moughadam S, Slemmon R, Van Kolen K, Theunis C, Mercken M, Kolb HC. Development and validation of a high-sensitivity assay for measuring p217+tau in plasma. *Alzheimer's Dement: Diagnosis Assessment Dis Monit.* 2021;13:e12204.
70. Groot C, Cicognola C, Bali D, Triana-Baltzer G, Dage JL, Pontecorvo MJ, Kolb HC, Ossenkoppele R, Janelidze S, Hansson O. Diagnostic and prognostic performance to detect Alzheimer's disease and clinical progression of a novel assay for plasma p-tau217. *Alzheimer's Res Ther.* 2022;14:67.
71. Ashton NJ, Pascoal TA, Karikari TK, Benedet AL, Lantero-Rodriguez J, Brinkmalm G, Snellman A, Schöll M, Troakes C, Hye A, et al. Plasma p-tau231: a new biomarker for incipient Alzheimer's disease pathology. *Acta Neuropathol.* 2021;141:709–24.
72. Milà-Alomà M, Ashton NJ, Shekari M, Salvadó G, Ortiz-Romero P, Montoliu-Gaya L, Benedet AL, Karikari TK, Lantero-Rodriguez J, Vanmechelen E, et al. Plasma p-tau231 and p-tau217 as state markers of amyloid- β pathology in preclinical Alzheimer's disease. *Nat Med.* 2022;28:1797–801.

73. Park JH, Cho S-J, Jo C, Park MH, Han C, Kim E-J, Huh GY, Koh YH. Altered TIMP-3 levels in the cerebrospinal fluid and plasma of patients with Alzheimer's disease. *J Personalized Med*. 2022;12:827.
74. Hoe HS, Cooper MJ, Burns MP, Lewis PA, van der Brug M, Chakraborty G, Cartagena CM, Pak DT, Cookson MR, Rebeck GW. The metalloprotease inhibitor TIMP-3 regulates amyloid precursor protein and apolipoprotein E receptor proteolysis. *J Neurosci*. 2007;27:10895–905.
75. Jia D, Wang F, Yu H. Systemic alterations of tricarboxylic acid cycle enzymes in Alzheimer's disease. *Front Neurosci*. 2023;17:1206688.
76. Sonntag K-C, Ryu W-I, Amirault KM, Healy RA, Siegel AJ, McPhie DL, Forester B, Cohen BM. Late-onset Alzheimer's disease is associated with inherent changes in bioenergetic profiles. *Sci Rep*. 2017;7:14038.
77. Jiao SS, Shen LL, Zhu C, Bu XL, Liu YH, Liu CH, Yao XQ, Zhang LL, Zhou HD, Walker DG, et al. Brain-derived neurotrophic factor protects against tau-related neurodegeneration of Alzheimer's disease. *Transl Psychiatry*. 2016;6:e907–e907.
78. Barroeta-Espar I, Weinstock LD, Perez-Nieves BG, Meltzer AC, Siao Tick Chong M, Amaral AC, Murray ME, Moulder KL, Morris JC, Cairns NJ, et al. Distinct cytokine profiles in human brains resilient to Alzheimer's pathology. *Neurobiol Dis*. 2019;121:327–37.
79. Wojcieszak J, Kuczyńska K, Zawilska JB. Role of chemokines in the development and progression of Alzheimer's disease. *J Mol Neurosci*. 2022;72:1929–51.
80. Wharton W, Kollhoff AL, Gangishetti U, Verble DD, Upadhyaya S, Zetterberg H, Kumar V, Watts KD, Kippels AJ, Gearing M, et al. Interleukin 9 alterations linked to Alzheimer disease in African Americans. *Ann Neurol*. 2019;86:407–18.
81. Kiyota T, Ingraham KL, Jacobsen MT, Xiong H, Ikezu T. FGF2 gene transfer restores hippocampal functions in mouse models of Alzheimer's disease and has therapeutic implications for neurocognitive disorders. *Proc Natl Acad Sci U S A*. 2011;108:E1339–1348.
82. Sathe G, Na CH, Renuse S, Madugundu AK, Albert M, Moghekar A, Pandey A. Quantitative proteomic profiling of cerebrospinal fluid to identify candidate biomarkers for Alzheimer's disease. *Proteom Clin Appl*. 2019;13:1800105.
83. Johnson ECB, Bian S, Haque RU, Carter EK, Watson CM, Gordon BA, Ping L, Duong DM, Epstein MP, McDade E, et al. Cerebrospinal fluid proteomics define the natural history of autosomal dominant Alzheimer's disease. *Nat Med*. 2023;29:1979–88.
84. Bader JM, Geyer PE, Müller JB, Strauss MT, Koch M, Leypoldt F, Koertvelyessy P, Bittner D, Schipke CG, Incesoy EI, et al. Proteome profiling in cerebrospinal fluid reveals novel biomarkers of Alzheimer's disease. *Mol Syst Biol*. 2020;16:e9356.
85. Esteve P, Rueda-Carrasco J, Inés Mateo M, Martín-Bermejo MJ, Draffin J, Pereyra G, Sandois Á, Crespo I, Moreno I, Aso E, et al. Elevated levels of Secreted-Frizzled-Related-Protein 1 contribute to Alzheimer's disease pathogenesis. *Nat Neurosci*. 2019;22:1258–68.
86. Bai B, Wang X, Li Y, Chen PC, Yu K, Dey KK, Yarbro JM, Han X, Lutz BM, Rao S, et al. Deep multilayer brain proteomics identifies molecular networks in Alzheimer's disease progression. *Neuron*. 2020;105:975–991. e977.
87. Abu-Rumeileh S, Steinacker P, Polisch B, Mammanna A, Bartoletti-Stella A, Oeckl P, Baiardi S, Zenesini C, Huss A, Cortelli P, et al. CSF biomarkers of neuroinflammation in distinct forms and subtypes of neurodegenerative dementia. *Alzheimers Res Ther*. 2019;12:2.
88. Baldacci F, Toschi N, Lista S, Zetterberg H, Blennow K, Kilimann I, Teipel S, Cavado E, dos Santos AM, Epelbaum S, et al. Two-level diagnostic classification using cerebrospinal fluid YKL-40 in Alzheimer's disease. *Alzheimers Dement*. 2017;13:993–1003.
89. Perez-Nieves BG, Stein TD, Tai HC, Dols-Icardo O, Scotton TC, Barroeta-Espar I, Fernandez-Carballo L, de Munain EL, Perez J, Marquie M, et al. Dissecting phenotypic traits linked to human resilience to Alzheimer's pathology. *Brain*. 2013;136:2510–26.
90. Tubi MA, Kothapalli D, Hapenny M, Feingold FW, Mack WJ, King KS, Thompson PM, Braskie MN. Regional relationships between CSF VEGF levels and Alzheimer's disease brain biomarkers and cognition. *Neurobiol Aging*. 2021;105:241–51.
91. De Kort AM, Kuiperij HB, Kersten I, Versleijen AAM, Schreuder F, Van Nostrand WE, Greenberg SM, Klijn CJM, Claassen J, Verbeek MM. Normal cerebrospinal fluid concentrations of PDGFR β in patients with cerebral amyloid angiopathy and Alzheimer's disease. *Alzheimers Dement*. 2022;18:1788–96.
92. Duits FH, Brinkmalm G, Teunissen CE, Brinkmalm A, Scheltens P, Van der Flier WM, Zetterberg H, Blennow K. Synaptic proteins in CSF as potential novel biomarkers for prognosis in prodromal Alzheimer's disease. *Alzheimer's Res Ther*. 2018;10:5.
93. Cicognola C, Mattsson-Carlgen N, van Westen D, Zetterberg H, Blennow K, Palmqvist S, Ahmadi K, Strandberg O, Stomrud E, Janelidze S, Hansson O. Associations of CSF PDGFR β with aging, blood-brain barrier damage, neuroinflammation, and Alzheimer disease pathologic changes. *Neurology*. 2023;101:e30–9.
94. Wang Y, Emre C, Gyllenhammar-Schill H, Fjellman K, Eijfjöldsdottir H, Eriksdotter M, Schultzberg M, Hjorth E. Cerebrospinal fluid inflammatory markers in Alzheimer's disease: influence of comorbidities. *Curr Alzheimer Res*. 2021;18:157–70.
95. Sudduth TL, Winder Z, Elahi FM, Nelson PT, Jicha GA, Wilcock DM. CSF and plasma placental growth factor as a biomarker for small-vessel damage in VCI. *Alzheimers Dement*. 2021;17:e052995.
96. Hinman JD, Elahi F, Chong D, Radabaugh H, Ferguson A, Maillard P, Thompson JF, Rosenberg GA, Sagare A, Moghekar A, et al. Placental growth factor as a sensitive biomarker for vascular cognitive impairment. *Alzheimers Dement*. 2023;19:3519–27.
97. Ashton NJ, Janelidze S, Al Khleifat A, Leuzy A, van der Ende EL, Karikari TK, Benedet AL, Pascoal TA, Lleó A, Parnetti L, et al. A multicenter validation study of the diagnostic value of plasma neurofilament light. *Nat Commun*. 2021;12:3400.
98. Bridel C, van Wieringen WN, Zetterberg H, Tijms BM, Teunissen CE, Group atN. Diagnostic value of cerebrospinal fluid neurofilament light protein in neurology: a systematic review and meta-analysis. *JAMA Neurol*. 2019;76:1035–48.
99. Balistreri CR, Monastero R. Neuroinflammation and neurodegenerative diseases: how much do we still not know? *Brain Sci*. 2023;14:19–38.
100. Zhang W, Xiao D, Mao Q, Xia H. Role of neuroinflammation in neurodegeneration development. *Signal Transduct Target Ther*. 2023;8:267.
101. Nelson AR, Sweeney MD, Sagare AP, Zlokovic BV. Neurovascular dysfunction and neurodegeneration in dementia and Alzheimer's disease. *Biochim Biophys Acta*. 2016;1862:887–900.
102. Müller N. The role of intercellular adhesion molecule-1 in the pathogenesis of psychiatric disorders. *Front Pharmacol*. 2019;10:1251.
103. Otgongerel D, Lee H-J, Jo SA. Induction of ICAM1 in brain vessels is implicated in an early AD pathogenesis by modulating neprilysin. *NeuroMol Med*. 2023;25:193–204.
104. Bui TM, Wiesolek HL, Sumagin R. ICAM-1: A master regulator of cellular responses in inflammation, injury resolution, and tumorigenesis. *J Leukoc Biol*. 2020;108:787–99.
105. Lawson C, Wolf S. ICAM-1 signaling in endothelial cells. *Pharmacol Rep*. 2009;61:22–32.
106. Lange C, Storkebaum E, de Almodovar CR, Dewerchin M, Carmeliet P. Vascular endothelial growth factor: a neurovascular target in neurological diseases. *Nat Rev Neurol*. 2016;12:439–54.
107. Yang H-S, Yau W-YW, Carlyle BC, Trombetta BA, Zhang C, Shirzadi Z, Schultz AP, Pruzin JJ, Fitzpatrick CD, Kirn DR, et al. Plasma VEGFA and PGF impact longitudinal tau and cognition in preclinical Alzheimer's disease. *Brain*. 2024;147:2158–68.
108. Bitto A, Lerner CA, Nacarelli T, Crowe E, Torres C, Sell C. p62/SQSTM1 at the interface of aging, autophagy, and disease. *Age*. 2014;36:1123–37.
109. Rubino E, Rainero I, Chiò A, Rogaeva E, Galimberti D, Fenoglio P, Grinberg Y, Isaia G, Calvo A, Gentile S, et al. *SQSTM1* mutations in frontotemporal lobar degeneration and amyotrophic lateral sclerosis. *Neurology*. 2012;79:1556–62.
110. Muto V, Flex E, Kupchinsky Z, Primiano G, Galehdari H, Dehghani M, Cecchetti S, Carpentieri G, Rizza T, Mazaheri N, et al. Biallelic *SQSTM1* mutations in early-onset, variably progressive neurodegeneration. *Neurology*. 2018;91:e319–30.
111. Weston LL, Jiang S, Chisholm D, Jantzie LL, Bhaskar K. Interleukin-10 deficiency exacerbates inflammation-induced tau pathology. *J Neuroinflammation*. 2021;18:161.
112. Hersh LB, Rodgers DW. Neprilysin and amyloid beta peptide degradation. *Curr Alzheimer Res*. 2008;5:225–31.

113. El-Amouri SS, Zhu H, Yu J, Marr R, Verma IM, Kindy MS. Neprilysin: an enzyme candidate to slow the progression of Alzheimer's disease. *Am J Pathol.* 2008;172:1342–54.
114. Campos CR, Kemble AM, Niewoehner J, Freskgård P-O, Urich E. Brain Shuttle neprilysin reduces central amyloid- β levels. *PLoS ONE.* 2020;15:e0229850.
115. Kim YS, Joh TH. Matrix metalloproteinases, new insights into the understanding of neurodegenerative disorders. *Biomol Ther (Seoul).* 2012;20:133–43.
116. Rosell A, Ortega-Aznar A, Alvarez-Sabín J, Fernández-Cadenas I, Ribó M, Molina CA, Lo EH, Montaner J. Increased brain expression of matrix metalloproteinase-9 after ischemic and hemorrhagic human stroke. *Stroke.* 2006;37:1399–406.
117. Kwon HS, Koh S-H. Neuroinflammation in neurodegenerative disorders: the roles of microglia and astrocytes. *Translational Neurodegeneration.* 2020;9:42.
118. Thakur S, Dhapola R, Sarma P, Medhi B, Reddy DH. Neuroinflammation in Alzheimer's disease: current progress in molecular signaling and therapeutics. *Inflammation.* 2023;46:1–17.
119. Zheng HT, Wu Z, Mielke MM, Murray AM, Ryan J. Plasma Biomarkers of Alzheimer's Disease and neurodegeneration according to sociodemographic characteristics and chronic health conditions. *J Prev Alzheimer's Dis* 2024. <https://doi.org/10.14283/jpad.2024.142>.
120. Mielke MM, Fowler NR. Alzheimer disease blood biomarkers: considerations for population-level use. *Nat Rev Neurol.* 2024;20:495–504.

Publisher's Note

Springer Nature remains neutral with regard to jurisdictional claims in published maps and institutional affiliations.